Anillin Mediates Feedback Between the Cortex and Microtubules to Define the Division Plane

Melina Jaramillo Garcia

A Thesis
in
The Department
of
Biology

Presented in Partial Fulfillment of the Requirements
for the Degree of Master of Science (Biology) at
Concordia University
Montreal, Quebec, Canada

August 2013

CONCORDIA UNIVERSITY

School of Graduate Studies

This is to certify that the thesis prepared

By: Melina Jaramillo Garcia

Entitled: Anillin Mediates Feedback Between the Cortex and Microtubules to Define the Division Plane

and submitted in partial fulfillment of the requirements for the degree of

Master of Science (Biology)

complies with the regulations of the University and meets the accepted standards with respect to originality and quality.

Signed by the final Examining Committee:

_____ Chair
Dr. Daniel McLaughlin

_____ External Examiner
Dr. Vladimir Titorenko

_____ Examiner
Dr. Catherine Bachewich

_____ Examiner
Dr. Gary Brouhard

_____ Examiner
Dr. William Zerges

_____ Supervisor
Dr. Alisa Piekny

Approved by _____
Dr. Selvadurai Dayanandan, Graduate Program Director

_____ 2013

_____
Joanne Locke, Interim Dean of Faculty

ABSTRACT

Anillin Mediates Feedback Between the Cortex and Microtubules to Define the Division Plane

Melina Jaramillo Garcia

Cytokinesis, the physical separation of a dividing cell into two daughter cells, is driven by the ingression of an actomyosin contractile ring. The mitotic spindle, which is composed of distinct populations of microtubules, dictates the location of the division plane. In particular, the central spindle, which forms between segregating sister chromatids recruits Ect2, the GEF leading to the activation of RhoA and the formation of the actomyosin ring in the equatorial plane. Anillin is a key regulator of cytokinesis that interacts with the core components of the division machinery including actin, myosin and their upstream regulator RhoA. Anillin also interacts with the membrane and proteins associated with the mitotic spindle. These numerous interactions stabilize the position of the ring to maintain the division plane. Consistent with this, anillin depletion causes lateral instability of the contractile ring and leads to mitotic failure. While the signaling pathway that activates RhoA from the central spindle is well understood, it is not known whether there is feedback from the cortex to the mitotic spindle to mediate changes in microtubule stability in response to cortical perturbations. Recently, *C. elegans* anillin was shown to directly interact with microtubules. Therefore, since anillin

interacts with both cortical components and microtubules, it is a good candidate for mediating feedback from the cortex to the spindle to stabilize subsets of microtubules that position the contractile ring.

Here, we investigate anillin-microtubule interactions in human (HeLa) cells. Anillin localizes to microtubules during mitosis, and this localization is enhanced after treatments that stabilize microtubules or decrease RhoA activation. Anillin also directly interacts with taxol-stabilized microtubules *in vitro*. In anillin-depleted cells, there is a decrease in the proportion of centrally located spindle microtubules and a loss of bundled microtubules in monopolar cells. Live imaging of stably expressing EB1:2EGFP cells show that in the absence of anillin, a pool of long microtubules that emanate toward the equatorial cortex are missing. Together, these results suggest that anillin's localization to microtubules could increase their stability, and supports a role for anillin in mediating feedback between the cortex and the mitotic spindle.

Acknowledgments and Dedications

I would like to thank first and foremost my supervisor, Dr. Alisa Piekny. Thank you Alisa for giving me the chance to pursue my master degree. You were a patient, encouraging and dedicated supervisor. You have taught me many scientific and life lessons that I will not forget. Under your mentorship, I have gained self-confidence and a renewed enthusiasm for biology. The last two years have been enjoyable and fulfilling.

Thank you to my committee members, Dr. Catherine Bachewich, Dr. Gary Brouhard and Dr. William Zerges for their precious advice, enthusiasm and expertise.

I would like to give a very special thanks to all the members of my lab. I now consider each and every one of you a friend. Madhav thank you for passing on your lab skills, for all the laughs, pranks and most of all your never-ending devotion to your lab mates. You are indispensible and “team-awesome” will definitely endure. Nellie, you were a spark of energy everyday, a model of work ethic and a great support. Chloë thank you for your wise guidance and for igniting my brand new passion for microscopy. Tara, your pep talks, optimism and our science conversations made my time in the lab even richer. Michelle, I feel privileged to have worked with an exceptional student and am glad to know you. Denise, thank you for your inexhaustible drive and your friendship. I am glad we started this journey together and happy you get to go on. Yun, I enjoyed our quiet talks early in the morning and thanks for letting me brush up my little Cantonese with you. Alexa, I

am sure I would have enjoyed working with someone so pleasant had we spent more time together in the lab. I would also like to thank Paul Frenette, Michael Loloyan, Husni Haji Bik and Mena Kinal for their help at the beginning of my project.

This endeavor would have not been possible without the constant support from my friends and family. Shaima, Monisha, Samar, Noor and Aisha, thank you all for believing in me even before I did. Jorge, Celeste, Angela, Luis-Gabriel and Javier: you are the best family one could ask for and inspire me to better myself everyday. I love you all dearly.

This would not be complete without a special thanks to all the babysitters that made it possible for me to go to work everyday with peace of mind. Dadi, Nana, Marinel, Maricel and Irene, I am sincerely grateful.

Last but not least, I would like to dedicate the first half of my thesis to my mother. You have been my strongest and most enthusiastic supporter and got me my first microscope when I was 10 years old. You saw my scientific streak before anyone else and nurtured it throughout the years. Your sacrifices and hard work are an example of strength and resilience I cherish everyday. This degree would not have been possible without you. The second part of my thesis is dedicated to the men in my life: my husband Aziz and my 3 year-old son, Mikaïl. Aziz you have been a pillar of strength and a source of constant love over the last 10 years. You have encouraged me and been present through the most difficult times and for that I am forever thankful. I am looking forward to the next 10 years... Mika, my little man, thank you for being such a good, patient boy and for bringing joy in my life everyday. I am looking forward to all the free hours I will get for playtime...

Contribution of Authors

Figure 3. This figure was obtained in collaboration with A. Piekny for slide preparation and image acquisition.

Figure 5. This figure was obtained in collaboration with H. Haji Bik (slide preparation and measurements) and A. Piekny (image acquisition).

Table of Contents

List of Figures..... x

Table of abbreviations..... xi

1. Introduction..... 1

1.1 Cytokinesis 1

1.2 The mitotic spindle and division plane..... 2

1.3 The central spindle..... 6

1.4 Anillin..... 8

2. Materials and Methods.....13

2.1 Cell culture and transfections.....13

2.2 RNAi and drug treatments.....13

2.3 Constructs.....15

2.4 Fixation and immunofluorescence.....16

2.5 Imaging of fixed cells.....17

2.6 Measurements and quantitation of fixed cell images.....18

2.7 Live Imaging of EB1:2EGFP.....19

2.8 Deconvolution and tracking of EB1:2EGFP movies.....20

2.9 Protein expression and purification.....21

2.10 Microtubule co-sedimentation assay.....23

2.11 Western Blotting.....24

3. Results.....26

3.1 Anillin-Microtubule interactions.....26

3.1.1 Anillin weakly localizes to microtubules in HeLa cells.....26

3.1.2 Anillin localizes to microtubules in the absence of active RhoA.....28

3.1.3 Anillin's cortical localization is competed by taxol-stabilized microtubules.....30

3.1.4 The CPC associates with taxol-stabilized microtubules.....32

3.1.5 Aurora B kinase may regulate anillin's association with taxol-stabilized microtubules.....36

3.1.6 Anillin directly interacts with taxol-stabilized microtubules *in vitro*.....39

3.2 Functional data.....41

3.2.1 Anillin is required for centrally located microtubules in HeLa cells.....41

3.2.2 Anillin is required for the stability of equatorial astral microtubules.....43

3.2.3 Anillin is required for spindle formation in monopolar HeLa cells.....45

4. Discussion.....49

4.1 Anillin localizes to microtubules in HeLa cells.....49

4.2 Anillin interacts directly with microtubules.....52

4.3 Anillin associates with microtubules in an Aurora B-dependent manner.....53

4.4 Anillin stabilizes a sub-set of microtubules during cytokinesis.....55

References.....59

List of Figures

1. A human cell at the onset of cytokinesis.....3
2. A schematic representation of anillin and its interacting partners.....9
3. Anillin weakly localizes to microtubules in HeLa cells.....27
4. Anillin localizes to microtubules in Ect2-depleted cells.....29
5. Taxol-stabilized microtubules compete for anillin's cortical localization.....31
6. The CPC associates with taxol-stabilized microtubules, but not centralspindlin.....33
7. Anillin's localization to taxol-stabilized microtubules is dependent on Aurora B kinase.....37
8. Anillin directly binds to microtubules *in vitro*.....40
9. Anillin depletion causes a decrease in microtubule fluorescence in HeLa cells.....43
10. Anillin stabilizes microtubules near the cortex during anaphase.....44
11. Anillin is required for the accumulation of central spindle proteins in monopolar cells.....47
12. Anillin-microtubule interactions provide feedback from the cortex to the central spindle.....50

Table of Abbreviations

AHD – Anillin homology domain

ANI-1 – Anillin isoform 1 (*C. elegans*)

Cdk1 – Cyclin dependent kinase 1

CPC – Chromosome passenger complex

Cyk4 – Cytokinesis defect 4 (human MgcRacGAP; *Drosophila* RacGAP50C)

DAPI - 4, 6-diamidino-2-phenylindole

DMEM – Dulbecco's Modified Eagle Medium

DMSO – Dimethyl sulfoxide

DTT – Dithiothreiol

EB1 – End-binding protein 1

Ect2 – Epithelial cell transformer sequence 2

FBS – Fetal bovine serum

GAP – GTPase activating protein

GEF – Guanine nucleotide exchange factor

GDP – Guanosine diphosphate

GFP – Green fluorescent protein tagged vector

GTP – Guanosine triphosphate

HeLa – Henrietta Lacks cervical cancer cell line

INCENP – Inner centromere protein

KIF4 – Kinesin family member 4 (also referred to as KIF4A)

MAPs – Microtubule associated proteins

MBP – Maltose binding protein

mDia2 – mammalian Diaphanous-formin related 2

MKLP1 – Mitotic kinesin like protein 1

NDS – Normal donkey serum

PH – Pleckstrin homology domain

Plk1 – Polo-like kinase 1

PBST – Phosphate buffer saline (Triton X)

PIPES – Piperazine-1,4-bis(2-ethanesulfonic acid)

PRC1 – Protein regulator of cytokinesis 1

RhoA – Ras homolog gene family, member A

RNAi – RNA interference

ROCK – Rho dependent kinase

SDS-PAGE – Sodium dodecyl sulfate polyacrylamide gel electrophoresis

TBST – Tris buffer saline (Triton X)

TCA – Trichloroacetic acid

Chapter 1. Introduction

Mitosis is the indispensable process that allows a single cell to divide into two genetically identical cells. Errors that occur during cell division have serious consequences for organisms. For example, problems with chromosome segregation can lead to polyploidy or aneuploidy, causing cancer and birth defects (Pfau & Amon 2012). Cytokinesis is the last step of mitosis and describes the process where a contractile actomyosin ring ingresses to physically separate the two daughter cells (Green et al. 2012). The mitotic spindle determines the division plane and is composed of different subsets of microtubules that restrict the localization of actomyosin to the equatorial plane.

1.1 Cytokinesis

Cytokinesis requires the activation of the small GTPase RhoA to regulate downstream effectors that form and ingress the contractile ring (Eggert et al. 2006). During anaphase, Ect2, the GEF (guanine nucleotide exchange factor) for RhoA, mediates the conversion of inactive RhoA-GDP to active RhoA-GTP in a narrow region at the equatorial cortex (Kimura et al. 2000; Piekny et al. 2005; Yüce et al. 2005; Bement et al. 2006). To accomplish this, Ect2 is recruited to the central spindle and overlying cortex where it is regulated by the cell cycle to ensure that contractile ring formation is coupled with the segregation of sister chromatids.

To form the contractile ring, RhoA-GTP activates Rho-dependent kinase (ROCK), which phosphorylates nonmuscle myosin II regulatory light chain to

promote the assembly of bipolar myosin filaments (Matsumura 2005; Piekny et al. 2005). RhoA-GTP also activates formins, which regulate the nucleation and polymerization of F-actin filaments (Piekny et al. 2005; Kovar 2006). Furthermore, active RhoA recruits the scaffolding protein anillin, which binds to actin and myosin by its N-terminus, and to membrane-associated septins via its C-terminus (Piekny & Maddox 2010). Septins are GTP-binding proteins that form hetero-oligomeric complexes in the form of filaments or rings (Kinoshita et al. 2002; Mostowy & Cossart 2012). It is not clear how these filamentous proteins are assembled into the ring, but their function likely is to crosslink the contractile apparatus to the overlying plasma membrane (Kinoshita et al. 1997; Piekny & Maddox 2010). The mechanism of ring constriction is thought to occur by the myosin-mediated sliding of anti-parallel F-actin filaments. This sliding is thought to progressively close the ring and simultaneously pull in the membrane to pinch the cell in two (Biron et al. 2005). Alternatively, changes in actin crosslinking and actin disassembly may be sufficient to mediate ingression (Ma et al. 2012).

1.2 The mitotic spindle and division plane

The precise placement of the contractile ring is crucial to ensure the integrity of cell division. The mitotic spindle segregates sister chromatids, but also provides cues that influence the position of the ring. The spindle is composed of the central spindle, as well as polar (dynamic) and equatorial (stable) astral microtubules (Figure 1; Glotzer 2009; Green et al. 2012). Classic experiments using glass needles

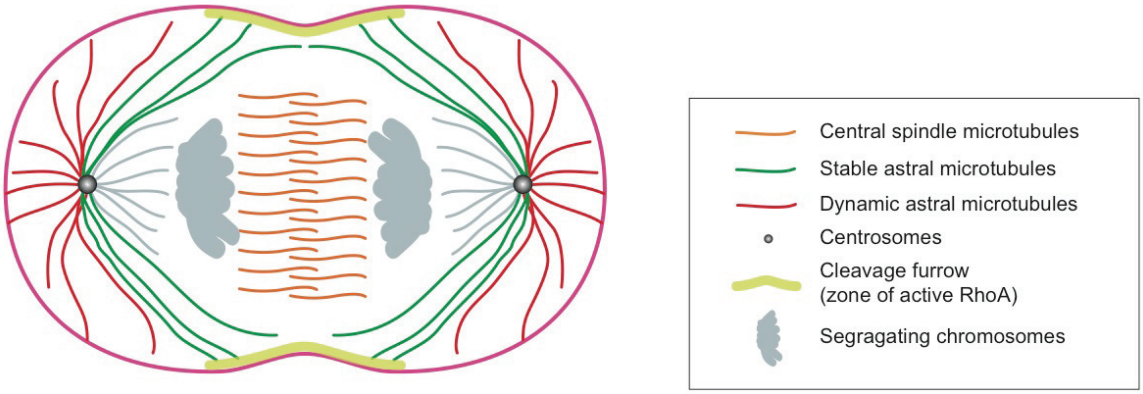

Figure 1. A human cell at the onset of cytokinesis

During anaphase/late telophase, the mitotic spindle is composed of different sub-populations of microtubules that have distinct roles in positioning the cleavage furrow (see legend). The central spindle, located between the segregating chromosomes, stimulates the generation of active RhoA in the overlying cortex. Stable astral microtubules that reach the equatorial plane contribute to furrow formation by being bundled by central spindle complexes and recruiting Ect2, the upstream activator of RhoA. At the cell poles, dynamic astral microtubules exclude the localization of contractile proteins required for furrow formation. The conjoint action of these pathways restricts the formation of the cytokinetic ring to a narrow equatorial region. *Note: This is an adapted figure from Green et al. (2012).*

to manipulate spindle position in echinoderm embryos showed that furrows always form in a position that bisect the mitotic spindle (Oegema & Mitchison 1997; Pollard 2004). These experiments were repeated using a probe for active RhoA, and showed that the zone of active RhoA always followed the new location of the spindle (Bement et al. 2005).

The key finding that a central spindle protein, MgcRacGAP (*C. elegans* CYK-4 or *Drosophila* RacGAP50C), can bind to and promote the activation of Ect2, provided molecular evidence for the role of the central spindle in stimulating contractile ring formation (Somers & Saint 2003; Piekny et al. 2005; Zhao & Fang 2005). In metaphase, Ect2 is phosphorylated by the master cell-cycle regulator Cdk1, which causes it to fold into an inactive conformation (Saito et al. 2003). At anaphase onset, this inhibitory phosphate is lost permitting Ect2 to form a complex with MgcRacGAP, hereafter referred to as Cyk4 (Yüce et al., 2005). The Cyk4/Ect2 interaction is also regulated by Polo-like kinase 1 (Plk1), which phosphorylates Cyk4 to generate a binding site for Ect2 (Petronczki et al. 2007; Wolfe et al. 2009). In support of this, inhibiting Plk1 causes cytokinesis phenotypes similar to Cyk4 or Ect2 depletion (Brennan et al. 2007; Burkard et al. 2007; Petronczki et al. 2007). The interaction between Cyk4 and Ect2 recruits the GEF to the central plane of the cell where it can generate active RhoA at the overlying equatorial cortex (Green et al. 2012).

Astral microtubules also help position the contractile ring, since furrow formation occurs in one-cell *C. elegans* embryos lacking a central spindle (Dechant & Glotzer 2003; Verbrugghe & White 2007; Lewellyn et al. 2010). Elegant studies in *C.*

elegans embryos revealed that both the central spindle and astral microtubules position the contractile ring (Dechant & Glotzer 2003; Bringmann & Hyman 2005; Lewellyn et al. 2010). First, astral microtubules prevent the accumulation of contractile proteins at the cell poles by promoting their removal or excluding them from the cortex. Mutant embryos that have more astral microtubules in the equatorial zone delay furrowing, while those with fewer astral microtubules generate ectopic furrows (Dechant & Glotzer 2003; Bringmann & Hyman 2005; Werner et al. 2007; Lewellyn et al. 2010; Tse et al. 2011). This data suggests that astral microtubules exclude contractile ring proteins from the poles and ensure their accumulation in the equatorial plane by default. This mechanism may be conserved, since treating mammalian cells with low doses of the microtubule-depolymerizing drug, nocodazole, causes the partial loss of astral microtubules and a broader zone of active RhoA (Murthy & Wadsworth 2008). The molecular mechanism that astral microtubules use to regulate the localization of contractile proteins has yet to be elucidated. Subsequent to the astral-mediated restriction of contractile proteins, the central spindle stimulates a dramatic increase in the levels of active RhoA to form a tight contractile ring. Removing the central spindle (while still permitting the formation of Cyk4/Ect2 complexes) causes contractile proteins to remain in a broad cortical zone in multiple cell types (Yüce et al. 2005; Werner et al. 2007; Lewellyn et al. 2010). These data support that several mechanisms position the contractile ring. The strength of one pathway vs. the other may vary depending on cell type and the size of their central spindle or astral microtubules. For example, in echinoderms and early *C. elegans* embryos, the astral microtubules are large and

dominate the cell, while in *Drosophila* and human cells the central spindle is more dominant.

Contrastingly, several groups showed that astral microtubules could also stimulate furrowing. Furrows can form between two adjacent asters from separate spindles in fused Ptk1 cells (Oegema et al. 2000). In *Drosophila* primary spermatocytes or echinoderm embryos, equatorial astral microtubules are bundled by central spindle complexes and likely contribute to the activation of RhoA (Inoue et al. 2004; Foe & von Dassow 2008). Similarly, in monopolar cells stimulated to exit mitosis, furrows form at positions that correspond to long astral microtubules decorated by central spindle associated complexes (Canman et al. 2003; Hu et al. 2008). Therefore, there are different pools of astral microtubules; dynamic and stable, and each may differentially regulate the localization of contractile proteins (Foe & von Dassow 2008). For example, dynamic astral microtubules that reach the poles prevent the accumulation of contractile proteins, while stable equatorial astral microtubules that reach the equatorial cortex promote the localization of contractile proteins.

1.3 The central spindle

The central spindle, also known as the spindle midzone, forms during anaphase, when antiparallel microtubules between segregating chromosomes are bundled with their plus ends pointing to the centre of the cell (Euteneuer & McIntosh 1980). These microtubules are tightly bundled by PRC1, an antiparallel microtubule crosslinker, which recruits the kinesin KIF4 to regulate the length of

the midzone microtubule overlap (Gaillard et al. 2008; Bieling et al. 2010). KIF4 depletion causes spindles to form that are twice as long as control cells, and these cells also have broader zones of active RhoA at the equatorial cortex (Hu et al. 2011). Additional complexes that regulate central spindle assembly are the centralspindlin complex and the chromosomal passenger complex (CPC) (Ruchaud et al. 2007; Carmena et al. 2009; Glotzer 2009). Disruption of either complex causes cytokinetic failure and lower levels of nonmuscle myosin II in the contractile ring (Adams & Maiato 2001; Glotzer 2005; Lewellyn et al. 2011). The CPC is composed of INCENP, Borealin and Survivin, which help localize and activate Aurora B kinase (Ruchaud et al. 2007; Carmena et al. 2009). The centralspindlin complex is a heterotetramer of MKLP1 (mitotic kinesin-like protein) and Cyk4 (Mishima et al. 2002; Mishima et al. 2004; Pavicic-Kaltenbrunner 2007). During anaphase, Aurora B-mediated phosphorylation of MKLP1 regulates its translocation towards the plus ends of microtubules, where it accumulates as a dotted line in the centre of the cell (Douglas et al. 2010). In human cells, inhibiting Aurora B in late anaphase causes late cytokinesis defects, but does not affect contractile ring formation or ingression (Guse et al. 2005; Yüce et al. 2005). Similarly, MKLP1 depletion often causes late cytokinesis phenotypes and *C. elegans* embryos carrying a mutation in the Aurora B phosphorylation site for ZEN-4 (MKLP1 homologue) also have late cytokinesis phenotypes (Guse et al. 2005). This suggests that Cyk4/Ect2 complexes still generate active RhoA at the equatorial cortex even if they are not recruited to the midzone in a focused manner by MKLP1 (Yüce et al. 2005; Nishimura & Yonemura 2006). These studies also show that there is crosstalk between centralspindlin and

the CPC. However, they may also function in separate pathways that contribute to contractile ring formation. For example, *C. elegans* embryos co-depleted for both a component of the CPC and centralspindlin display enhanced cytokinesis phenotypes (Lewellyn et al. 2011).

1.4 Anillin

As mentioned earlier, active RhoA recruits the scaffold protein anillin to the division site (Piekny & Maddox 2010). Anillin was first isolated from *Drosophila* embryonic extracts as an F-actin binding protein that localizes to contractile structures such as the contractile ring (Field & Alberts 1995). Anillin also interacts with other components of the contractile apparatus and its regulators, including active nonmuscle myosin II and the formin mDia2 via its N-terminus, and Ect2 (human) or RacGAP50C (*Drosophila*), RhoA, and membrane-associated septins through its C-terminus (Figure 2; Piekny & Maddox 2010). One of anillin's main functions is to crosslink actin and myosin, since anillin depletion in *Drosophila* and human cells causes an oscillation phenotype, where the ring is destabilized and cytokinesis fails (Straight et al. 2005; Hickson & O'Farrell 2008; Piekny & Glotzer 2008). Although the N- and C-terminus of anillin independently localize to the furrow, both halves are essential for anillin function (Piekny & Glotzer 2008; Kechad et al. 2012) .

An interaction between the Pleckstrin Homology (PH) domain at the very C-terminus of anillin and a hetero-oligomer of septins 2, 6 and 7 was demonstrated *in vitro* using *Xenopus laevis* mitotic extracts (Kinoshita et al. 2002). Importantly, the

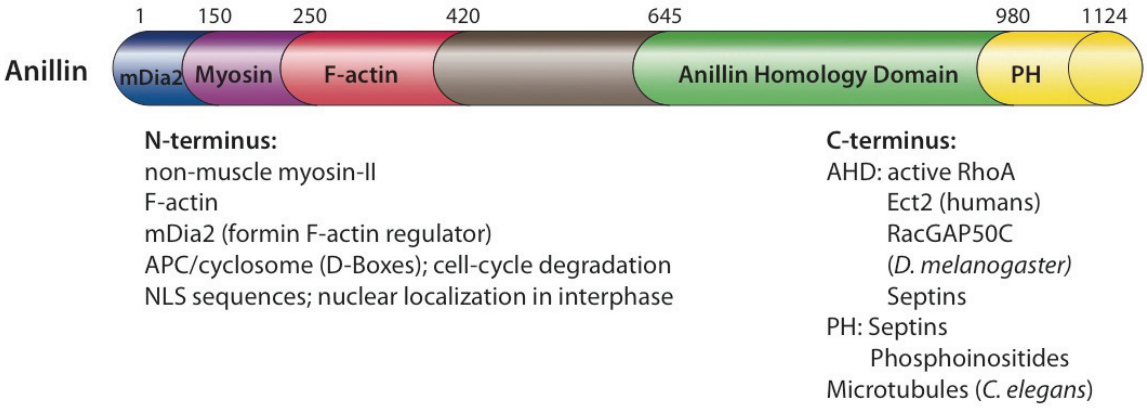

Figure 2. A schematic representation of anillin and its interacting partners

Anillin interacts with many components of the division machinery. The N-terminal of anillin interacts with non-muscle myosin-II, F-actin, mDia2 and contains D-boxes (sequences that mediate ubiquitination and degradation) and NLS sequences (sequences involved in the nuclear sequestration of anillin during interphase). The C-terminal end of anillin contains the AHD and PH domains, which can interact with active RhoA, Ect2 or Cyk4, septins, phosphoinositides PI(4,5)P_2, and microtubules. The two halves of anillin connect the cytokinetic ring to both the plasma membrane and the mitotic spindle. *Note: This figure was adapted Piekny and Maddox (2010).*

organization of F-actin was altered in the presence of both anillin and septins (Kinoshita et al. 2002). The interdependence between anillin and septins for their localization and organization is not well understood. Septins are a key component of contractile rings, and anillin, by virtue of its interactions with both F-actin and septins, could organize septin filaments along actin bundles (Kinoshita et al. 2002). In some organisms, anillin is required for septin localization, but not vice versa (e.g. *C. elegans* embryos) (Maddox et al. 2005; Maddox et al. 2007). However, mutations in anillin that disrupt septin binding cause phenotypes in *Drosophila* and human cells (Field et al. 2005; Piekny & Glotzer 2008). Since both septins and anillin can interact with phospholipids, their interaction could anchor the contractile ring to the plasma membrane (Tanaka-Takiguchi et al. 2009; Bertin et al. 2010; Estey et al. 2010; Liu et al. 2012).

Anillin binds to RhoA and Ect2 via the anillin-homology domain (AHD) in its C-terminus. Active RhoA recruits anillin to the contractile ring, however, depletion of anillin causes a decrease in the localization of active RhoA at the equatorial cortex (Zhao & Fang 2005; Piekny & Glotzer 2008), and its overexpression may increase the levels of RhoA-GTP (Suzuki et al. 2005). Anillin's interaction with Ect2 may be part of this feedback mechanism. Since Ect2 also binds to Cyk4 at the central spindle, its interaction with anillin may crosslink the central spindle to the overlying cortex to mediate the efficient activation of RhoA (Frenette et al. 2012). In support of this, central spindle microtubules are no longer stabilized near the cortex in the absence of anillin or Ect2 (Frenette et al. 2012). In *Drosophila* cells, anillin does not bind to the Ect2 homologue Pebble, but binds directly to RacGAP50C (Cyk4

homologue) and anillin depletion also causes a decrease in cortically associated microtubules (D'Avino et al. 2008; Gregory et al. 2008; Frenette et al. 2012).

Intriguingly, anillin also may interact with microtubules themselves (Sisson et al. 2000; Tse et al. 2011; Haji Bik and Piekny, unpublished observations). *Drosophila* anillin has an affinity for both F-actin and microtubules (Sisson et al. 2000) and *C. elegans* anillin (ANI-1) binds to purified microtubules *in vitro* and colocalizes with astral microtubules *in vivo* (Tse et al. 2011). Previous studies in our lab, using co-sedimentation assays with crude human cell extracts and colocalization assays, suggest that human anillin may also interact with microtubules in mammalian cells (Haji Bik and Piekny, unpublished observations). Furthermore, anillin may function with astral microtubules to regulate the organization of contractile proteins at the polar cortex in both *C. elegans* embryos and in human cells (Tse et al. 2011; Haji Bik, van Oostende and Piekny, unpublished observations).

Here, we further investigate the relationship between anillin and microtubules in cultured HeLa cells. More specifically, we determined if anillin directly binds to microtubules, and if this interaction is essential for cytokinesis. I found that human anillin directly interacts with microtubules, similar to the *C. elegans* homologue, ANI-1. Furthermore, during mitosis, anillin's localization with microtubules is enhanced in cells with low levels of active RhoA or in cells treated with the microtubule-stabilizing drug, taxol (Paclitaxel). Interestingly, anillin's interaction with taxol-stabilized microtubules is Aurora B-dependent, suggesting that Aurora B phosphorylation may mediate anillin's interaction with microtubules.

In addition, a pool of microtubules near the equatorial cortex is lost in anillin-depleted cells, and microtubules are no longer polarized or bundled in anillin-depleted monopolar cells. Furthermore, using a probe that marks the plus ends of microtubules, I found that anillin is required for microtubule stability *in vivo*. These results suggest that anillin may mediate feedback between the cortex and the mitotic spindle to ensure that the division plane can shift in response to perturbations.

Chapter 2. Materials and Methods

2.1 Cell culture and transfections

HeLa cells were cultured and maintained in Dulbecco's Modified Eagle Medium (DMEM; Wisent), supplemented with 10% fetal bovine serum (FBS; Thermo Scientific), 2 mM L-glutamine, 100 U penicillin and 0.1 mg/mL streptomycin (Wisent). Cells were kept in a humidified incubator with 5% CO_2 at 37°C. For transfection, HeLa cells were plated on coverslips in 6-well dishes in DMEM without antibiotics. Cells were transfected with short interference RNAs using Oligofectamine (Invitrogen) according to manufacturer's instructions (except that 9-12 µL of Oligofectamine was used per 2 -3 mL of media). For optimal RNAi transfection, cells were transfected at ~50% confluency, and the media was replaced by the siRNA mixture and minimal essential medium (Opti-MEM; Invitrogen) for 4-5 hours. The mixture was then replaced with DMEM containing FBS and glutamine as described above, and left for an additional 25-30 hours. For optimal DNA transfection, cells were transfected at 50-80% confluency (depending on the constructs) with Lipofectamine (Invitrogen) according to manufacturer's instructions, except that ~4-5 µL of Lipofectamine was used per 2-3 mL of media (e.g. one well of a six-well dish) and cells were collected for imaging or fixing after 24 hours.

2.2 RNAi and drug treatments

The following siRNA duplexes were used to target various genes as

previously described: Ect2, GGCGGAAUGAACAGGAUUU (1.6 nM); MKLP1, CGACAUAACUUACGACAAAUU (2.0 nM); and Anillin, CGAUGCCUCUUUGAAUAAA (1.6 nM; ThermoScientific; Yüce et al. 2005; Piekny & Glotzer 2008).

Synchronization experiments were performed as previously described (Yüce et al. 2005). Cells were treated with 2.5 mM thymidine (dissolved in sterile water) (Bioshop) for 12-16 hours, then washed with 3-4 volumes of phosphate saline buffer (1X, 137 mM NaCl, 2.7 mM KCl, 10 mM NA_2HPO_4 and 1.8 mM $KH2PO_4$, pH 7.4, without calcium or magnesium; Wisent), after which pre-warmed DMEM media containing FBS was added to the cells. At this point, the cells were transfected with RNAi if required. After a total of 8 hours of release, thymidine was added again for 12 hours. To obtain synchronized interphase cells, they were kept in thymidine. To synchronize cells for mitosis, they were released (after 3-4 washes with 1X PBS and adding DMEM with FBS) for 6 hours, then 2 μM of S-trityl-L-cysteine (STC; Sigma-Aldrich) was added for 4-6 hours to accumulate cells in prometaphase. Cells were released by washing 3-4 times with 1X PBS, then left for 30 minutes to obtain metaphase cells, or 60 minutes to obtain anaphase cells. To perform monopolar assays, STC-arrested cells were treated with 22.5 μM Purvalanol A (Sigma-Aldrich) for 20-25 minutes before fixing.

For taxol treatments, 10 μM taxol (Bioshop) was added to the media for 20 minutes (or 10-40 min for the time course), then the media was removed and the cells were washed and fixed. To inhibit Aurora B kinase, 100 nM of hesperadin (Boehringer Mannheim) was added to taxol-treated cells for 30 minutes prior to

their fixation. All drugs were dissolved in DMSO as 1000X stocks except hesperadin, which was dissolved in PBS.

2.3 Constructs

The EB1:2EGFP DNA construct was kindly provided by Dr. Torsten Wittman (UCSF, CA, USA). A HeLa cell line stably expressing EB1:2EGFP was generated using G418 (Wisent) selection followed by dilution cloning. HeLa cells were transfected with 2-6 μg of DNA using Lipofectamine. After 24 hours, plates were washed with 1X PBS, then pre-warmed media containing FBS was added to the cells with 100 μL of G418 (100 mg/mL) for the first 'kill' (where non-expressing cells die due to the G418). The surviving cells were trypsinized (400 μL 1X trypsin; Wisent) and diluted by a factor of 10,000 into 10 cm plates containing pre-warmed media with FBS. The diluted cells were grown for 24-48 hours in the presence of G418 (50 μL). Positive clones were screened by fluorescence microscopy and a small piece of sterile Whatman paper soaked in trypsin was added to the desired clone. After 30-60 seconds, the cells were transferred into 12-well dishes containing fresh DMEM media with FBS. Cells were grown for another 24-48 hours in the presence of G418, then checked for viability and fluorescence before being frozen in freezing media (10% DMSO, 50% FBS and 40% DMEM) using a specialized freezing container with a cooling rate of -1°C/min (Mr. Frosty freezing container, Thermo Scientific). When the cells reached -80°C, they were flash frozen and stored in liquid nitrogen.

2.4 Fixation and immunofluorescence

Cells were grown on glass coverslips (washed with 0.1 M HCl, then sterilized with isopropanol and air-dried under sterile hood) and washed in pre-warmed (37°C) cytoskeletal buffer (80 mM PIPES, 1 mM $MgCl_2$, 5 mM EGTA). The cells were fixed in 100% ice-cold MeOH (stored at -20°C) for 20 minutes (to stain for DM1A tubulin, anillin, myosin, MKLP1, Aurora B, Ect2, INCENP, Cyk4 or Plk1) or 10% w/v ice-cold trichloroacetic acid (TCA; prepared 30 minutes before use from a fresh 100% stock) for 15 minutes (to stain for RhoA and anillin). Subsequently, cells were washed 3-4 times with 1X TBST buffer (0.5% Triton X-100, 0.15 M NaCl and 0.05 M Tris, pH 7.4). The following antibodies and dilutions were used: 1:50 mouse anti-Plk1 antibodies (Santa Cruz), 1:200 rabbit anti-anillin antibodies (Piekny & Glotzer 2008), 1:100 rabbit anti-Ect2 antibodies (Yüce et al. 2005), 1:200 mouse anti-tubulin antibodies (DM1A, Sigma-Aldrich), 1:100 rabbit anti-nonmuscle myosin II antibodies (Sigma-Aldrich), 1:100 rabbit anti-MKLP1(Mishima et al. 2002), 1:100 mouse anti-Aurora B (BD Transduction Laboratories), 1:100 rabbit anti-INCENP (Santa Cruz), 1:100 mouse anti-Cyk4 (Abnova) and 1:50 mouse anti-RhoA (Santa Cruz). The following secondary antibodies were used at 1:350 dilutions: anti-mouse or anti-rabbit Alexa 488 and anti-mouse or anti-rabbit Alexa 568 (Invitrogen). After fixing, the coverslips were placed in a wet chamber (a covered plastic dish with wet paper towels to prevent drying) and cells were blocked with 5% NDS (Normal Donkey Serum) in TBST for 20 minutes. Immunostaining was performed by incubating cells with primary antibodies diluted in TBST with 5% NDS for 2 hours at room temperature. Cells were washed 3 times with TBST and treated with

secondary antibodies diluted in TBST with 5% NDS for 2 hours at room temperature. Cells were washed 2 times with TBST before adding 1:1000 DAPI (4, 6-diamidino-2-phenylindole; 1 mg/mL; Sigma-Aldrich) in TBST for 5 minutes. Cells were washed one last time with TBST before washing once with 0.1 M Tris pH 8.8. The Tris was removed and a drop of mounting media (4% n-propyl gallate in 50% glycerol, 0.1 M Tris pH 8.8) was added to the coverslip, which was then placed onto a glass slide. Excess liquid was wicked away using a Kimwipe (Kimtech), then the coverslip was sealed with nail polish.

2.5 Imaging of fixed cells

Fixed cells were imaged with a Leica DMI6000B inverted microscope (Leica Microsystems) using 40X/ 0.75 NA or 63X/ 1.4 NA oil immersion objectives and a Hamamatsu digital CCD OrcaR2 camera with Volocity acquisition software (PerkinElmer). For localization or quantitation, 0.2–0.5 μm Z-stacks were acquired using a Piezo Z stage (Mad City Labs). For all images, exposure times were kept below 4000 levels to avoid signal saturation. For measurements on bipolar and monopolar cells, exposure times (300-500 msec) and gain levels (~120) were kept within the same range for control and treatment slides. Images were opened and converted into maximum intensity Z-stack projections using the Java-based software Image J (NIH) before being measured or imported into Illustrator CS5 (Adobe).

2.6 Measurements and quantitation of fixed cell images

For tubulin measurements in bipolar cells, maximum intensity Z-stack projections of cells co-stained for myosin and tubulin were generated using Image J. Measurements of the total intensity of tubulin were performed using elliptical shapes in the central region of the cell between segregating chromosomes, as shown in Figure 9A. Myosin was used to mark the cell cortex and to determine the location of cell boundaries. Cells were matched for mitotic stage by observing the distance between segregating chromosomes and DNA condensation. Intensities were averaged for control and RNAi treated cells (control n= 23, anillin RNAi n = 19, MKLP1 RNAi n = 17 and Ect2 RNAi n = 17 cells) and plotted on a bar graph using Excel (Microsoft).

Standard deviations were calculated by Excel (Microsoft) using the following formula:

$$s = \sqrt{\frac{\sum(x - \bar{x})^2}{n - 1}}$$

Where s = standard deviation; x = Individual value; $\bar{x}$ = mean; and n = number of values.

The student's t-test was calculated by Excel (Microsoft) using the following formula:

$$t = \frac{\overline{x_1} - \overline{x_2}}{\sqrt{\frac{S_1^2}{N_1} + \frac{S_2^2}{N_2}}}$$

Where $\overline{x1}$ = Mean of first set of values x; $\overline{x2}$ = Mean of second set of values; S_1 =

Standard deviation of first set of values; S_2 = Standard deviation of second set of values; n_1 = Total number of values in first set; and n_2 = Total number of values in second set.

To quantitate the number of Plk1 foci in monopolar cells, maximum intensity Z-stack projections of cells co-stained for anillin and Plk1 were generated using Image J. Control cells were selected based on polarization of the cortex (anillin accumulation on one side of the cortex). Ect2-depleted cells were selected based on the cytoplasmic and microtubule localization of anillin, as well as by DNA position and shape (after mitotic exit, DNA is positioned at the opposite side of the polarized cortex and adopts a "peanut" shape). Anillin and MKLP1-depleted cells were screened for the absence of anillin or its cytosolic localization and comparing the position and shape of DNA. For each cell, the number of Plk1 foci near the cortex were counted manually (Figure 11). The Plk1 foci associated with kinetochores (overlapping with the DNA signal) were not counted (Figure 11). The number of foci were averaged for each condition (control n = 38 cells, anillin RNAi n = 24, Ect2 RNAi n = 35, MKLP1 RNAi n = 23, Anillin + Ect2 RNAi n = 29, and Ect2 + MKLP1 RNAi n = 22) and plotted on a bar graph using Excel (Microsoft).

2.7 Live imaging of EB1:2EGFP cells

Cells stably expressing EB1:2EGFP were plated on a 25 mm round coverslip (No. 1.5) and placed in a 35 mm Chamlide magnetic chamber (Quorum). Imaging

was performed at 37°C in 5% CO_2 using an inverted Nikon Eclipse Ti microscope with a Piezo Z stage (Prior), a 100X/1.45 NA oil immersion objective, and a Livescan Swept Field confocal unit (Prairie) with the iXON897 EMCCD camera (Andor) and Elements acquisition software (4.0 Nikon). Cells were filmed from anaphase through furrow ingression. To obtain images with optimal GFP levels, 70 ms exposures with the 488 nm laser (100 mW, Agilent) at 30%, and 11 Z-stacks of 0.5 μm were taken per cell. Anillin RNAi-treated cells were matched to control cells using the position of segregating DNA, and were filmed longer (e.g. additional 15 minutes) to confirm cytokinetic failure (single Z-slice, 100 msec exposure time, every 30 sec).

2.8 Deconvolution and tracking of EB1:2EGFP movies

To increase the signal/noise ratio, EB1:2EGFP movies were imported as ND2 files into Autoquant X software (Media Cybernetics) and images were deconvolved using a point spread function (PSF) customized for the NIKON Ti Sweptfield. To create the PSF, slides were prepared using fluorescent micro-beads (FluoSpheres®, Invitrogen). First, a 1:1000 dilution of the microbeads in H_20 was vortexed for 5 min. Next, a second dilution of 1/100 of beads and water was made (final dilution of 1/100 000) and vortexed for another 5 min. A clean coverslip was pre-washed in ethanol, dried and flamed (to get an hydrophilic surface). Then, 5 uL of the diluted beads was placed on the coverslip, spread evenly across, and dried for 1-2 h. A small drop of water was placed on a pre-cleaned slide. The coverslip was then mounted on the slide and sealed with nail polish. The slide was left to settle before imaging with

the Nikon Ti Sweptfield using the same settings as the EB1:2EGFP movies. A field of beads was imaged by collecting 0.1 μm Z stacks. Images were transferred into Autoquant X where a PSF was automatically calculated and used for deconvolution.

Manual tracking of EB1 was performed using 3D-projections of deconvolved EB1:2EGFP movies in IMARIS software (Bitplane). EB1 comets near the equatorial cortex (within the area of interest in control and anillin-depleted cells outlined in Figure 10) were tracked from their first appearance. Typically, 10-40 tracks were followed for each cell depending on the phenotype and intensity of the signal. IMARIS-generated track statistics were exported into Excel spreadsheets (Microsoft). Track length (μm) and duration (msec) were categorized as shown in Figure 10B for each cell, and averaged for control (n=10) and anillin-depleted cells (n=14). Due to glitches in the NIS Elements software, we suspect that real time metadata was not properly assigned to the movies. For these reasons, the duration was calculated by averaging the frame gap time (total time in msec/total number of frames) and converting the number of frames for each track into msec. Results were compiled into bar graphs using Excel (Microscoft). Standard deviations and student t-tests were calculated as described in section 2.6.

2.9 Protein expression and purification

Anillin C-terminus (608-1087) and N-terminus (100-460) fragments previously cloned into the pMAL vector (NEB) and transformed into *E. coli* (BL21)

were grown in 5 mL LB Amp (1% NaCl, 1% Tryptone, 0.5% yeast extract in H_2O, pH 7.0; 0.1 mg/mL ampicillin) cultures overnight. The next day, they were diluted into 300 mL LB Amp cultures and grown with shaking at 37°C until they reached an OD^{600} of 0.4-0.6. To induce protein expression, 0.5 mM IPTG was added to the cultures and they were grown with shaking for another 5 hours at 29°C. Then, the cells were pelleted by centrifugation at 4,000 rpm for 15 minutes and washed with 1 X PBS pH 7.2 (137 mM NaCl, 2.7 mM KCl, 10 mM NA_2HPO_4 and 1.8 mM KH_2PO_4) for C-term or 1 X TBS pH 7.5 (2.5 mM $MgCl_2$, 50 mM Tris, 150 mM NaCl) for N-term. After washing and centrifugation, the pellets were flash frozen in liquid nitrogen, and placed at -20°C overnight. The next day, bacterial pellets were thawed on ice and re-suspended in 30 mL PBST (1 X PBS with 0.5% Tween-20) or TBST (1 X TBS with 0.5% Tween-20) supplemented with DTT (1 mM; Amresco), PMSF (1 mM; Bio Basics) and a protease inhibitor cocktail (Roche). Lysozyme (1 µg/mL; Bio Basics) was added and cells were left on ice for 30 minutes before being sonicated on ice (30% amplitude, 3 X 1 min; 1 sec on and 1 sec off). Bacterial debris was pelleted by centrifugation at 10,000 rpm for 20 min at 4°C, then the supernatant was collected and bound to 300 µL of equilibrated (same buffer as above for each protein) amylose resin (NEB) at 4°C for 5 hours with rotating. The bound beads were collected by centrifugation at 4,000 rpm for 10 min at 4°C. They were subsequently washed 3-4 X with 500 µL PBS or TBS (see above; centrifuged at 4,000 rpm for 5 min at 4°C after each wash). After the last wash, the majority of the buffer was removed to generate a 50% w/v bead slurry. The bound beads were stored at 4°C until needed (maximum of 2 weeks). The MBP fusion proteins were eluted by

removing the buffer from the bound beads, then adding 250 µL of maltose (100 mM; Bioshop) to the beads and incubating them on ice for 2 hours with gentle mixing. The beads/maltose mixtures were centrifuged at 4,000 rpm for 5 min at 4°C and the supernatants containing the eluted proteins were removed from the beads. Additional maltose was added to the beads and the above was repeated to ensure that any remaining protein was eluted (elutions were kept separate and stored at 4°C). Aliquots of the eluted proteins were run by SDS-PAGE with a known standard (1 µg of BSA) and gels were stained with Coommassie Blue, destained and scanned to calculate protein concentration based on pixel intensity using Image J (NIH).

2.10 Microtubule co-sedimentation assay

Lyophilized bovine brain microtubules (500 µg; Cytoskeleton) were reconstituted in 3 mL of PM buffer (15 mM PIPES pH 7.0, 1 mM $MgCl_2$) containing 20 µM taxol for 10-15 min at room temperature (final concentration, 9.1 µM), then 60 µL aliquots were made in microcentrifuge tubes, which were flash frozen in liquid nitrogen. Frozen microtubules were left to thaw on the bench until they reached room temperature. Purified anillin proteins also were warmed to room temperature on the bench just prior to adding them to the microtubules. For the co-sedimentation assays, reaction volumes of 25 µL were set up in 200 µL polycarbonate tubes (Beckman Coulter). Each reaction contained 2.5 µM microtubules in BRB80 buffer (80 mM PIPES, pH 6.8, 1 mM EGTA, and 1 mM $MgCl_2$) supplemented with 1 mM DTT and 10 µM taxol, and 0.5 µM anillin proteins (1:4

ratio to the microtubules). Control reactions lacked either the microtubules, or the anillin proteins. The reactions were incubated at room temperature for 30 minutes. The reactions were then ultracentrifuged at 90,000 rpm for 5 minutes, with 10 minutes deceleration (Beckman Coulter Optima MAX Ultracentrifuge, Rotor TLA-100). Both the supernatant and pellet fractions were recovered, and equal volumes of pellet and supernatant were loaded and resolved by SDS-PAGE (12 % acrylamide). Gels were stained in Coomassie Blue, destained, and scanned with a digital scanner.

2.10 Western blotting

Hela cells were grown on 6 cm culture plates and synchronized for interphase, metaphase and anaphase as described in section 2.2. Control, anillin or Ect2-depleted cells were lysed using a cell scraper with 200 µL TBST (2.5 mM $MgCl_2$, 50 mM Tris pH 7.5, 150 mM NaCl and 0.5% Triton-X) supplemented with 1 mM DTT, 1 mM PMSF and protease inhibitors (Roche) on ice. The lysates were centrifuged at 12,000 rpm at 4°C for 5 minutes, then the supernatants were collected and aliquots were incubated with sample buffer. Denatured samples were run by SDS-PAGE (12% acrylamide), which was then transferred onto a nitrocellulose membrane (GE Healthcare). The membrane was stained with Ponceau S to check for optimal transfer. After washing off the Ponceau stain with water, the membrane was blocked for 20 minutes with 5% w/v skim milk in PBST (1X PBS with 0.2% Tween-20). Then, the blot was incubated with 1:2,500 mouse anti-tubulin antibodies (DM1A,

Sigma-Aldrich) in PBST for 1-2 hours at room temperature with gentle rocking. The membrane was subsequently washed 3 X with PBST for 5-10 minutes per wash, then incubated with a 1:3,500 dilution of anti-mouse Alexa 488 antibodies in PBST. The membrane was then washed 3 X with PBST, and scanned using the 488 nm laser on the Typhoon Trio Multi-mode Imager (optimized to keep the signal below saturation).

Chapter 3. Results

3.1 Anillin-Microtubule interactions

3.1.1. Anillin weakly localizes to microtubules in HeLa cells

Anillin has a dynamic localization pattern during the cell cycle. Before mitotic entry, anillin is enriched in the nucleus, and during mitosis it localizes to the contractile ring and subsequently to the midbody (Field & Alberts 1995). In *Drosophila* cells, anillin also localizes to midbody microtubules (D'Avino et al. 2008; Gregory et al. 2008) and in *C. elegans* embryos, the anillin homologue, ANI-1, is enriched on microtubule structures near the cortex (Tse et al. 2011). To determine if human anillin also localizes to microtubules during mitosis, we examined fixed HeLa cells co-stained for anillin (green) and RhoA (red), or anillin (green) and tubulin (red; Figure 3). In metaphase, anillin was cytoplasmic and weakly localized to astral microtubules (red arrows; Figure 3). Anillin's localization to microtubules in metaphase cells could be part of a sequestration mechanism to prevent the accumulation of contractile proteins to the cortex prior to anaphase [Haji Bik, van Oostende and Piekny, unpublished observations]. Anillin remained localized to astral microtubules in early anaphase (red arrows; Figure 3), but it also weakly localized to the cortex (Figure 3). During late anaphase (before furrow ingression) and early telophase (during furrow ingression), anillin was strongly enriched at the cleavage furrow and colocalized with RhoA (Figure 3A). In telophase cells (after

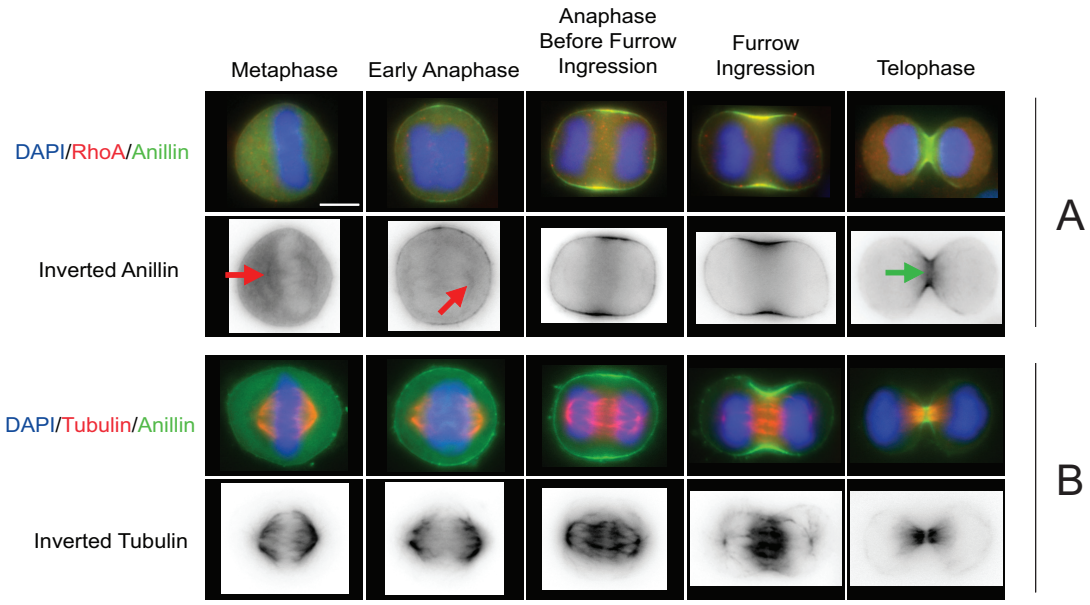

Figure 3. Anillin weakly localizes to microtubules in HeLa cells.

A) Z-stack projections of TCA fixed HeLa cells co-stained for RhoA (red), anillin (green), and DNA (DAPI; blue). Different cells are shown for the various mitotic stages as indicated above the panels. The corresponding inverted anillin images show the changes in anillin localization as cells progress through mitosis. Red arrows point to anillin associated with astral microtubules in metaphase and early anaphase cells. The green arrow points to the localization of anillin to the central spindle microtubules in telophase. B) Z-stack projections of methanol fixed HeLa cells co-stained for tubulin (red), anillin (green), and DNA (DAPI, blue). Inverted tubulin images show changes in the mitotic spindle as cells progress through mitosis. The scale bar is 10 μm. *Note: this figure was obtained in collaboration with A. Piekny for slide preparation and image acquisition.*

furrow ingression), anillin localized to the furrow remnant (also called the midbody) and was visible on central spindle microtubules (green arrow; Figure 3). Anillin's localization pattern suggests that it could interact with microtubules during mitosis, likely when the levels of active RhoA are low.

3.1.2 Anillin localizes to microtubules in the absence of active RhoA

In control mitotic cells, anillin's colocalization with microtubules seems to correspond to rising and dropping levels of active RhoA at the equatorial cortex (Figure 3A). To determine if there is competition between anillin's microtubule and cortical localization, we reduced the levels of active RhoA by depleting its GEF, Ect2, and fixed and co-stained these cells for anillin (green) and tubulin (red; Figure 4). In Ect2 RNAi cells, anillin's localization in metaphase and early anaphase was similar to control cells. However, during anaphase and telophase, anillin's localization to central spindle microtubules was enhanced in comparison to control cells (Figures 3 and 4) and very little anillin localized to the equatorial cortex (inverted anillin; Figure 4). Therefore, anillin localizes to microtubules in the absence of active RhoA, at the expense of its localization to the equatorial cortex. These results support a model where there is competition between active RhoA and microtubules for anillin localization. Interestingly, in the Ect2-depleted cells, the central spindle microtubules appeared to be more bundled (inverted tubulin; Figure 4) compared to control cells (Figure 3B). An interesting hypothesis is that anillin could also have a role in microtubule bundling, particularly during midbody formation.

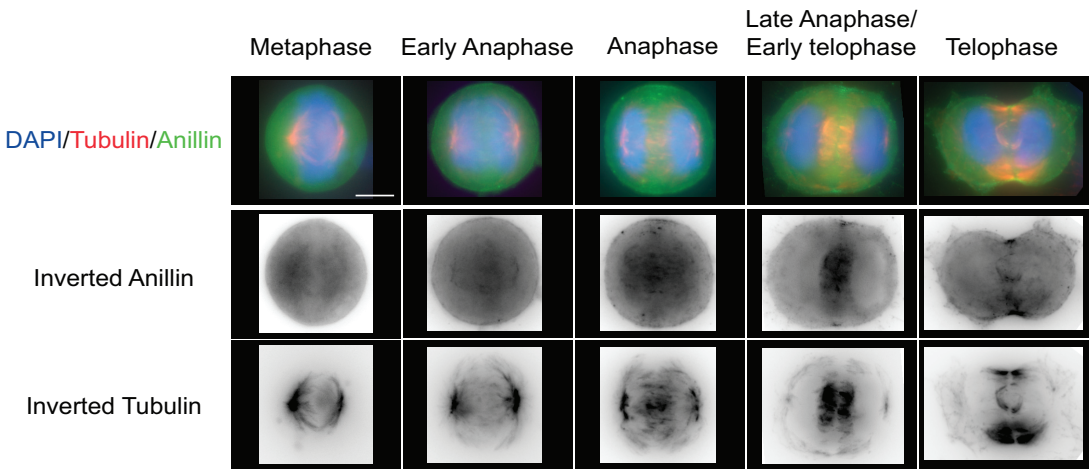

Figure 4. Anillin localizes to microtubules in Ect2-depleted cells

Z-stack projections of methanol fixed HeLa cells treated with Ect2 RNAi co-stained for anillin (green), tubulin (red) and DNA (DAPI; blue). The various stages of mitosis are indicated above the panels. The corresponding inverted anillin and tubulin images are shown for each stage of mitosis. In the absence of active RhoA, anillin does not localize to the equatorial cortex and is enriched on microtubules. The scale bar is 10 μm.

3.1.3 Anillin's cortical localization is competed by taxol-stabilized microtubules

Anillin weakly localizes to microtubules in HeLa cells, and strongly localizes to central spindle microtubules when the levels of active RhoA are reduced after Ect2 depletion. Central spindle microtubules are less dynamic compared to other populations of microtubules within the spindle (Salmon et al. 1984; Saxton et al. 1984). Therefore, we hypothesized that anillin could have a higher affinity for stable microtubules in comparison to more dynamic microtubules. To test this hypothesis, cells were treated with taxol, a microtubule-stabilizing drug, then fixed and co-stained for anillin (red) and tubulin (green; Figure 5). Taxol prevents both polymerization and depolymerization of microtubules by binding to the β tubulin subunit along the interior of the microtubule lattice (Jordan & Wilson 2004). At moderate concentrations (10 μM), taxol "freezes" the spindle microtubules by suppressing their dynamic instability (Derry et al. 1995). The microtubules of taxol-treated cells reorganized over time, as shown by the aggregation of minus ends and separation of the midzone overlap (tubulin; Figure 5A). Strikingly, in taxol-treated cells, anillin was increasingly enriched on microtubules over time, which occurred at the expense of its cortical localization (anillin; Figure 5A). This change in anillin localization in taxol-treated cells was quantitated by measuring the average ratio of anillin fluorescence intensity at the equatorial cortex in comparison to anillin's fluorescence inside the cell (including regions that contain mitotic spindle microtubules; Figure 5B). Anillin was significantly reduced at the equatorial cortex after 20 minutes of taxol-treatment in comparison to control cells (Figure 5B). This

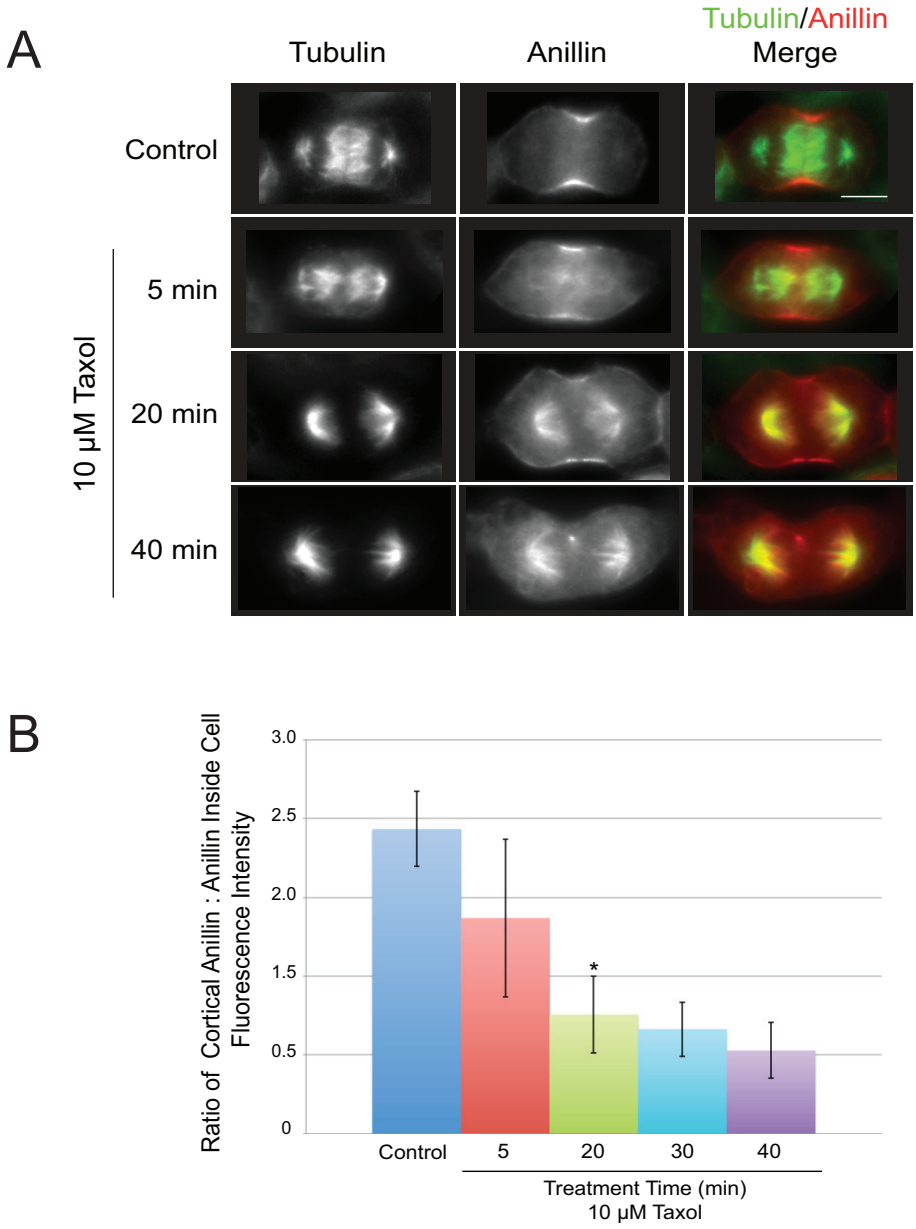

Figure 5. Taxol-stabilized microtubules compete for anillin's cortical localization

A) Z-stack projections of methanol fixed HeLa cells treated with 10 µM of taxol for varying lengths of time, co-stained for anillin (red) and tubulin (green). All cells shown are in early telophase. Anillin is at the equatorial cortex in control cells and is increasingly displaced onto taxol-stabilized microtubules over time. Taxol also causes reorganization of the mitotic spindle as shown by the tubulin staining. The scale bar is 10 µm. B) A bar graph shows the average ratio of anillin fluorescence intensity at the equatorial cortex vs. anillin 'inside the cell' (including regions of the cell where microtubules are enriched). The black bars show the standard deviations for each data set. After 20 minutes, the ratio is statistically significantly different from the control set, as per the student t-test ($p<0.01$). *Note: this figure was obtained in collaboration with H. Haji Bik (slide preparation and measurements) and A. Piekny (image acquisition).*

suggests that stabilized microtubules compete for anillin's cortical localization. As described in Chapter 1, anillin is part of a positive feedback loop that recruits additional active RhoA to the equatorial cortex (Suzuki et al. 2005; Zhao & Fang 2005; Piekny & Glotzer 2008; Frenette et al. 2012). Supporting this, previous work in our lab showed that the displacement of anillin onto taxol-stabilized microtubules prevented the accumulation of active RhoA at the equatorial cortex (Haji Bik and Piekny, unpublished observations). Therefore, the removal of anillin from the cortex can affect the localization of other contractile proteins and their regulators. Interestingly, our lab also previously found that septins localized with taxol-stabilized microtubules and this localization may be anillin-dependent [Haji Bik, unpublished observations]. This data suggests that anillin can form either distinct complexes, or have different affinities for septins vs. RhoA.

3.1.4 The CPC associates with taxol-stabilized microtubules

Since anillin may have a high affinity for taxol-stabilized microtubules, we sought to better characterize these microtubules. To do this, we fixed early telophase Hela cells treated with 10 μM taxol for 20 minutes, and co-stained for different central spindle proteins (Figure 6). Ect2 (green) and centralspindlin proteins (Cyk4; red and MKLP1; green) did not colocalize with taxol-stabilized microtubules (tubulin; red), and instead remained in the centre of the cell at the former location of the central spindle (Figure 6A). As cells progress through mitosis, the centralspindlin complex could 'precipitate' and be left behind as the microtubules stabilize and recede toward the poles (Mishima et al. 2002).

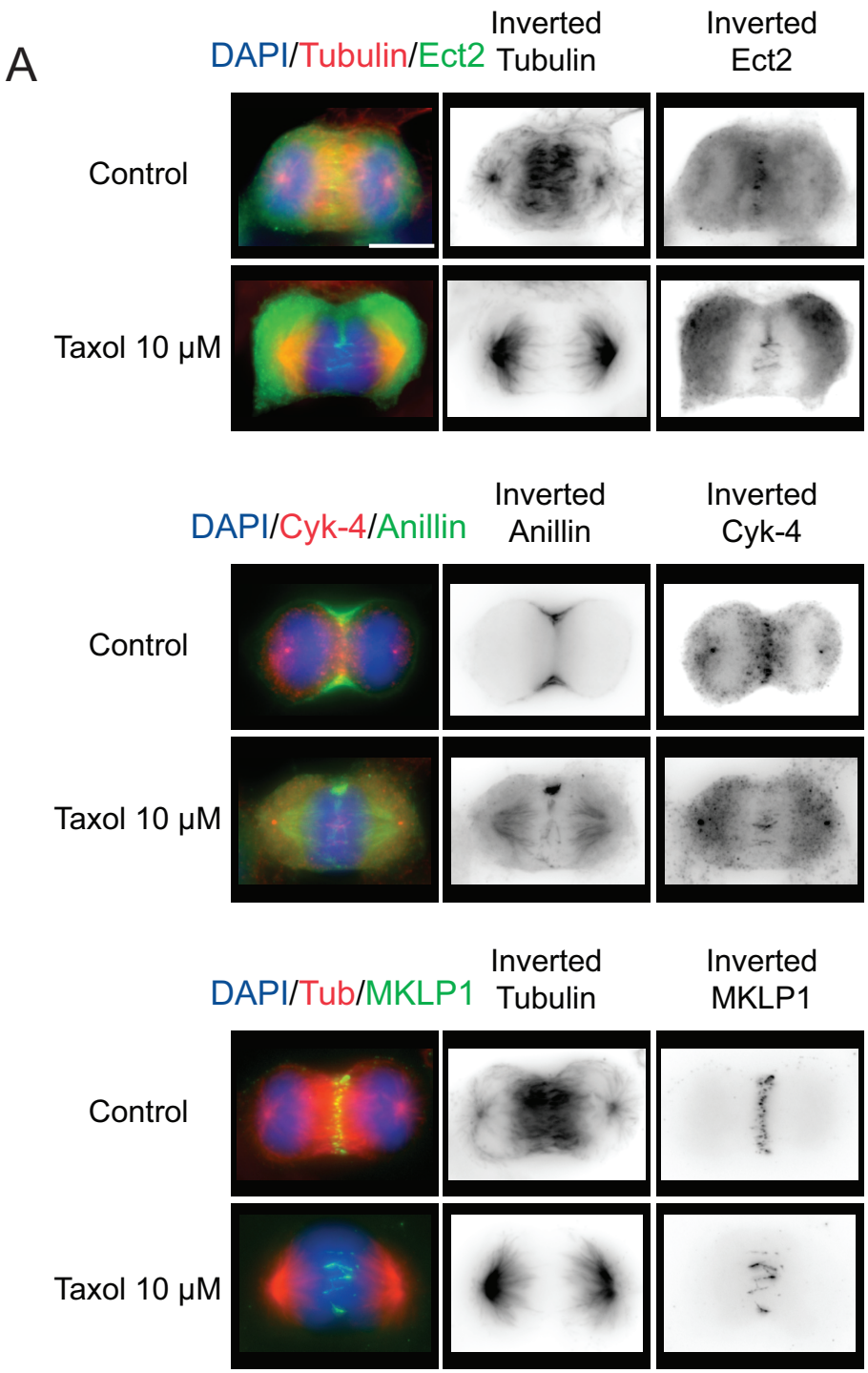
A
DAPI/Tubulin/Ect2
Inverted Tubulin
Inverted Ect2
Control
Taxol 10 μM
DAPI/Cyk-4/Anillin
Inverted Anillin
Inverted Cyk-4
Control
Taxol 10 μM
DAPI/Tub/MKLP1
Inverted Tubulin
Inverted MKLP1
Control
Taxol 10 μM

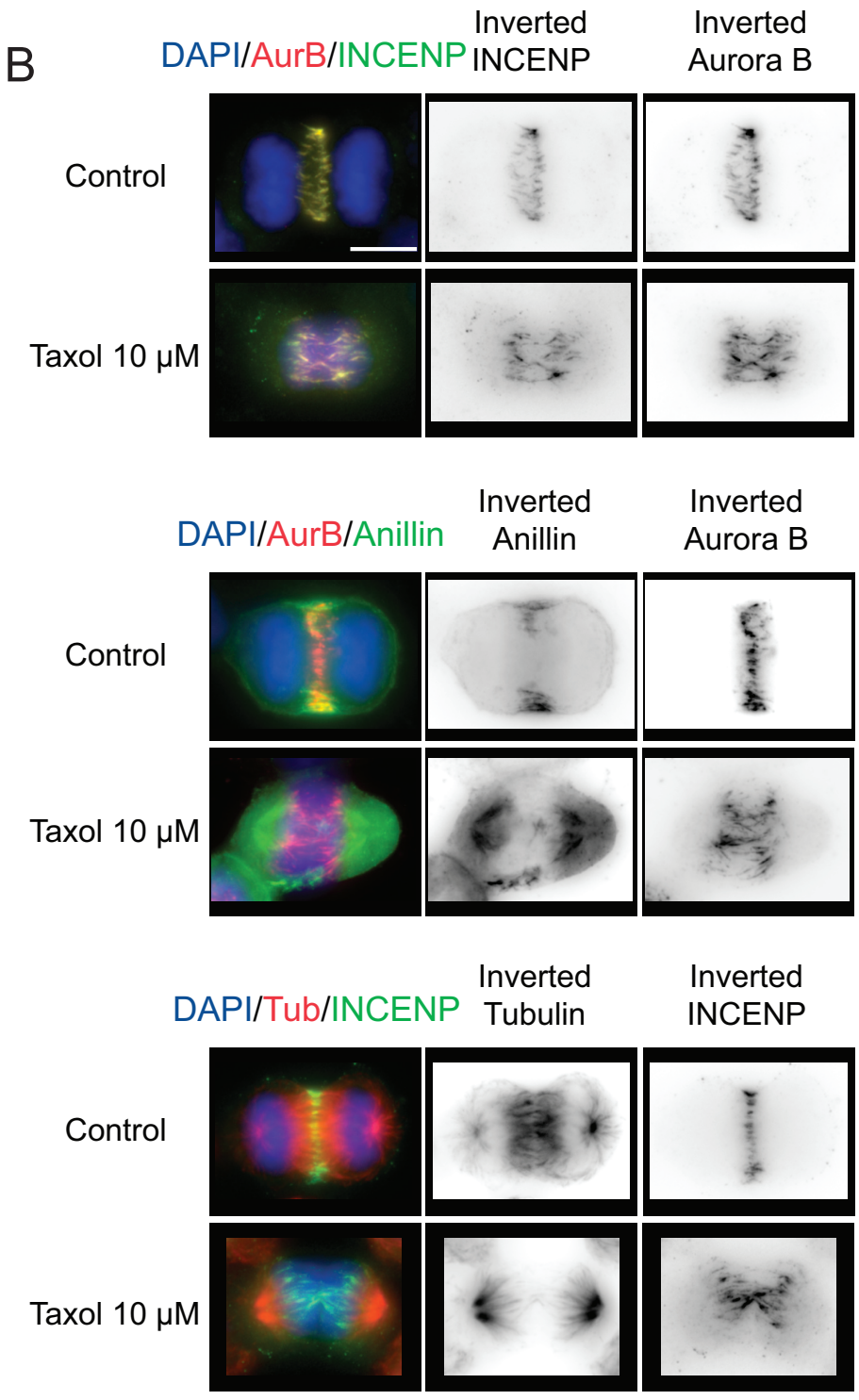

Figure 6. The CPC associates with taxol-stabilized microtubules, but not centralspindlin.

A) Z-stack projections of control and taxol-treated methanol-fixed HeLa cells (10 μM for 20 minutes) co-stained for Ect2 (green) and tubulin (red), or anillin (green) and Cyk4 (red), or MKLP1 (green) and tubulin (red), and

DAPI (DNA; blue). Ect2 and the centralspindlin complex remain in the central region of the cell and do not localize to the microtubules in taxol-treated cells. B) Z-stack projections of control and taxol-treated methanol-fixed HeLa cells (10 μM for 20 minutes) co-stained for INCENP (green) and Aurora B (red), or anillin (green) and Aurora B (red), or INCENP (green) and tubulin (red), and DAPI (DNA; blue). The CPC components remain associated with each other after taxol treatment, and although some pools remain centrally localized, their localization aligns with the plus ends of stable microtubules. The scale bar is 10 μm.

Interestingly, components of the CPC, Aurora B (red) or INCENP (green) displayed a different pattern of localization vs. centralspindlin in taxol-treated cells. Although pools of INCENP and Aurora B remained in the centre of the cell after taxol treatment, elongated foci of CPC were also observed at the plus ends of the microtubules (Figure 6B). Some of these foci may be associated with kinetochores, but other foci appear to align with the plus tips of microtubules. Aurora B and INCENP colocalized before and after treatment, suggesting that taxol does not cause this complex to dissociate (Figure 6B). The overlap between the plus ends of taxol-stabilized microtubules, anillin and the CPC suggest that anillin's association with stabilized microtubules could be regulated (in part) by the CPC.

3.1.5 Aurora B kinase may regulate anillin's association with taxol-stabilized microtubules

Anillin localizes to taxol-stabilized microtubules, and its localization overlaps with the CPC at the tips of microtubules (Figure 6). To determine if anillin's localization to taxol-stabilized microtubules is regulated by the CPC, we treated cells with taxol, then added the Aurora B kinase inhibitor, hesperadin (100 nM) (Sessa et al. 2005), and co-stained the cells for anillin (green) and tubulin (red; Figure 7A). After hesperadin treatment, anillin localized to the equatorial cortex and was no longer visible on microtubules (Figure 7A). Anillin appeared to be more broadly localized in hesperadin-treated cells in comparison to control HeLa cells (Figure 7A). This is consistent with previous studies showing that RhoA and other

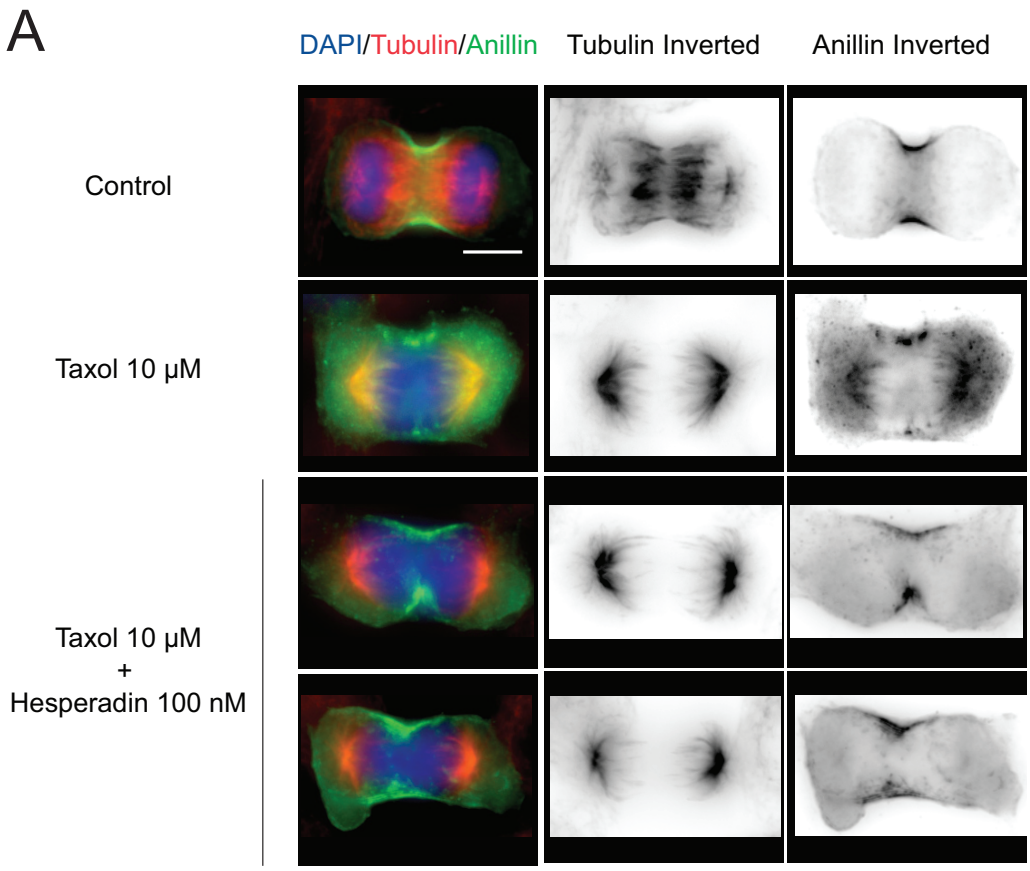

B

```
1     MDPFTEKLLE RTRARRENLQ RKMAERPTAA PRSMTHAKRA RQPLSEASNQ QPLSGGEEKS
61    CTKPSPSKKR CSDNTEVEVS NLENKQPVES TSAKSCSPSP VSPQVQPQAA DTISDSVAVP
121   ASLLGMRRGL NSRLEATAAS SVKTRMQKLA EQRRRWDNDD MTDDIPESSL FSPMPSEEKA
181   ASPPRPLLSN ASATPVGRRG RLANLAATIC SWEDDVNHSF AKQNSVQEQP GTACLSKFSS
241   ASGASARINS SSVKQEATFC SQRDGDASLN KALSSSADDA SLVNASISSS VKATSPVKST
301   TSITDAKSCE GQNPELLPKT PISPLKTGVS KPIVKSTLSQ TVPSKGELSR EICLQSQSKD
361   KSTTPGGTGI KPFLERFGER CQEHSKESPA RSTPHRTPII TPNTKAIQER LFKQDTSSST
421   THLAQQLKQE RQKELACLRG RFDKGNIWSA EKGGNSKSKQ LETKQETHCQ STPLKKHQGV
481   SKTQSLPVTE KVTENQIPAK NSSTEPKGFT ECEMTKSSPL KITLFLEEDK SLKVTSDPKV
541   EQKIEVIREI EMSVDDDDIN SSKVINDLFS DVLEEGELDM EKSQEEMDQA LAESSEEQED
601   ALNISSMSLL APLAQTVGVV SPESLVSTPR LELKDTSRSD ESPKPGKFQR TRVPRAESGD
661   SLGSEDRDLL YSIDAYRSQR FKETERPSIK QVIVRKEDVT SKLDEKNNAF PCQVNIKQKM
721   QELNNEINMQ QTVIYQASQA LNCCVDEEHG KGSLEEAEAE RLLLIATGKR TLLIDELNKL
781   KNEGPQRKNK ASPQSEFMPS KGSVTLSEIR LPLKADFVCS TVQKPDAANY YYLIILKAGA
841   ENMVATPLAS TSNSLNGDAL TFTTTFTLQD VSNDFEINIE VYSLVQKKDP SGLDKKKKTS
901   KSKAITPKRL LTSITTKSNI HSSVMASPGG LSAVRTSNFA LVGSYTLSLS SVGNTKFVLD
961   KVPFLSSLEG HIYLKIKCQV NSSVEERGFL TIFEDVSGFG AWHRRWCVLS GNCISYWTYP
1021  DDEKRKNPIG RINLANCTSR QIEPANREFC ARRNTFELIT VRPQREDDRE TLVSQCRDTL
1081  CVTKNWLSAD TKEERDLWMQ KLNQVLVDIR LWQPDACYKP IGKP
```

Aurora B kinase consensus sequence: R/K X S/T

Figure 7. Anillin's localization to taxol-stabilized microtubules is dependent on Aurora B kinase

A) Z-stack projections of control, taxol and taxol + hesperadin treated HeLa cells (10 μM taxol for 20 min and 100 nM hesperadin for 30 min) fixed in methanol and co-stained for anillin (green), tubulin (red) and DNA

(DAPI; blue). All cells are in early telophase. Anillin is at the cleavage furrow in control cells, on microtubules after taxol treatment and is at the equatorial cortex after hesperadin treatment. The scale bar is 10 μm. B) The amino acid sequence of full-length anillin is shown with consensus Aurora B phosphorylation sites (R/K X S/T, where X is any residue) highlighted in blue. The pink box marks a potential Aurora B site surrounded by a stretch of polybasic residues.

contractile proteins are restricted by central spindle microtubules (Yüce et al. 2005). Since Aurora B inhibition disrupted anillin's microtubule localization, this suggests that Aurora B may modulate anillin's affinity for microtubules. The amino acid sequence of full-length anillin revealed many potential sites that contain the core consensus sequence, R/K X S/T, for Aurora B phosphorylation (Figure 7B;Cheeseman et al. 2002; Ozlü et al. 2010). Another student in the lab found that the C-terminus of anillin localizes to taxol-stabilized microtubules, suggesting that the microtubule-interacting region for anillin is in the C-terminus (Haji Bik and Ricci, unpublished observations). Indeed, one site in the C-terminus is particularly attractive due to its surrounding stretch of basic residues (Figure 7B; isoelectric point of 10.82, *Innovagen peptide property calculator*). Since microtubule-binding domains are known to be polybasic, one hypothesis is that Aurora B phosphorylation at this site could change anillin's affinity for microtubules (Cravchik et al. 1994).

3.1.6 Anillin directly interacts with taxol-stabilized microtubules *in vitro*

To determine if human anillin's interaction with microtubules is direct, we performed co-sedimentation assays using pre-polymerized taxol-stabilized microtubules (Figure 8). Recombinant full-length anillin is difficult to purify, and previous experiments suggested that the C-terminus mediates anillin's interaction used either MBP-tagged N-terminus (100-460) or C-terminus of anillin (608-1087) to do the co-sedimentation assays. As shown in Figure 6, although the N-terminus of

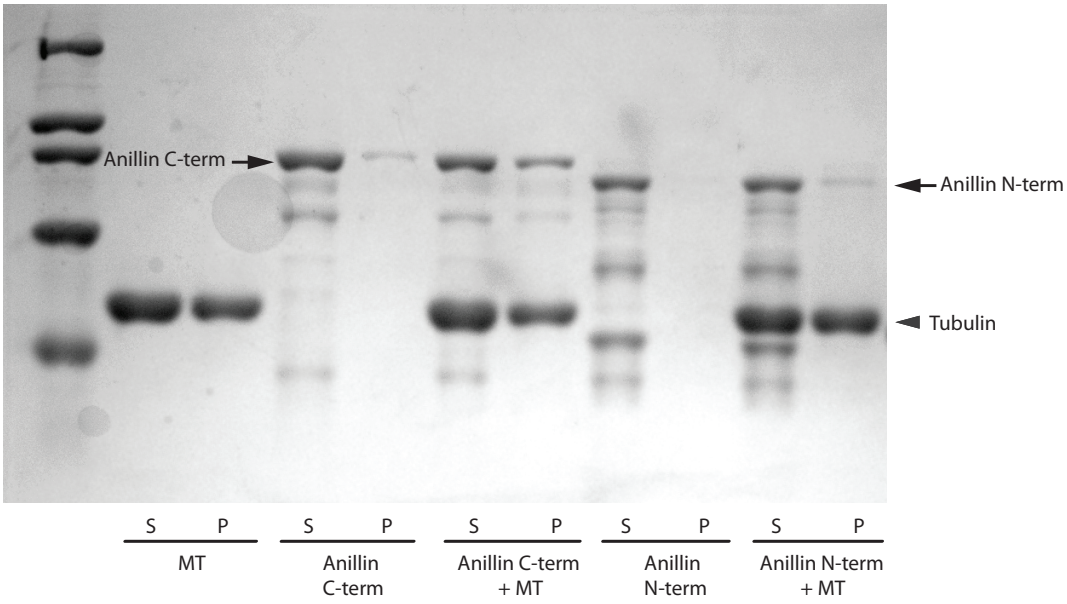

Figure 8. Anillin directly binds to microtubules *in vitro*.

A coomassie-blue stained SDS-PAGE gel shows the supernatant (S) and pellet (P) fractions of co-sedimentation assays with anillin proteins and taxol-stabilized microtubules (MT) *in vitro*. Purified, recombinant MBP-tagged C-terminus and N-terminus of anillin were centrifuged on their own, or after incubation with taxol-stabilized microtubules. The C-terminus more strongly interacts with microtubules in comparison to the N-terminus.

anillin weakly co-sedimented with microtubules, the C-terminus of anillin bound more strongly to microtubules. Another student in our lab found that MBP alone does not co-sediment with microtubules [Ricci, unpublished observations], thus the binding of the C-terminus of anillin to microtubules likely is not due to the MBP-tag. This data is consistent with previous studies showing that the *C. elegans* anillin homologue, AN1-1, also binds to microtubules *in vitro* (Tse et al. 2011).

3.2 Functional data

3.2.1 Anillin is required for centrally located microtubules in HeLa cells

Anillin directly binds to microtubules *in vitro* and colocalizes with microtubules *in vivo*. However, the function of the anillin-microtubule interaction is not clear. We previously showed that anillin may be required to anchor or stabilize a subset of microtubules near the cortex (Frenette et al. 2012). To determine if anillin is required for microtubule stability, we treated cells with anillin RNAi, then measured changes in tubulin fluorescence (Figure 9). We also depleted Ect2, previously shown to also affect the cortical localization of microtubules, and MKLP1, which is required for central spindle formation (Mishima et al. 2002; Frenette et al. 2012). The average total tubulin fluorescence between segregating chromosomes was measured using Z-stack projections of fixed cells stained for tubulin (Figure 9A and 9B). Cells lacking anillin showed a decrease in tubulin fluorescence in comparison to control or Ect2-depleted cells, although it was not as severe as

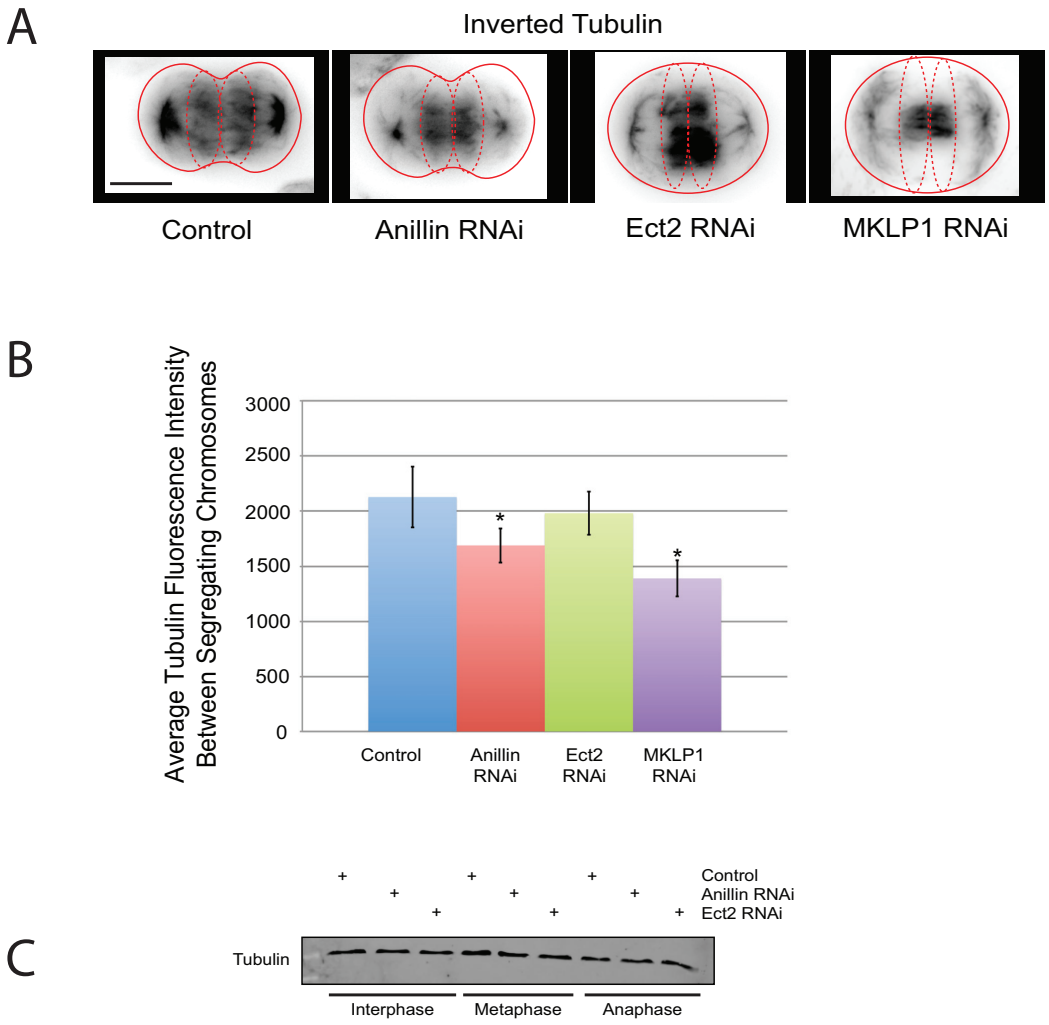

Figure 9. Anillin depletion causes a decrease in microtubule fluorescence in HeLa cells.

A) Z-stack projections of methanol-fixed HeLa cells treated with anillin, Ect2 or MKLP1 RNAi, co-stained for tubulin (inverted images shown) and anillin or myosin (as a cortical marker, not shown). The cells are in telophase, and are outlined by the red lines. The areas measured for total tubulin fluorescence are indicated by the red dashed lines. B) A bar graph shows the average intensity of tubulin fluorescence for cells from each treatment (n=17 to 23). The black bars show standard deviation. *Statistically significant from control cells as per the student t-test (p<0.01). The total intensity of tubulin is lower in MKLP1 and anillin-depleted cells in comparison to control or Ect2-depleted cells. C) A western blot of lysates from synchronized cells in interphase, metaphase and anaphase, after anillin or Ect2 RNAi and probed for tubulin. There is no obvious difference in the total tubulin levels in control cells vs. anillin and Ect2-depleted cells.

MKLP1-depleted cells (Figure 9B). This loss was not due to changes in the overall expression levels of tubulin, as shown by a western blot of cells for various stages of the cell cycle (Figure 9C). This suggests that anillin is required for maintaining microtubules in the central region of the cell, and could promote microtubule stability during cytokinesis. Interestingly, this requirement for anillin may be RhoA-independent, since the levels of tubulin fluorescence were unchanged after Ect2 depletion.

3.2.2 Anillin is required for the stability of equatorial astral microtubules

As described above, anillin may be required for microtubule stability. To better characterize anillin's effect on microtubules, we generated a line of HeLa cells stably expressing EB1:2EGFP and compared the dynamics of microtubules in control vs. anillin-depleted cells (Figure 10). EB1 is a plus-end microtubule associated protein that associates with polymerizing microtubules, but not with depolymerizing microtubules (Morrison et al. 1998; Mimori-Kiyosue et al. 2000). The average speed of comets for control and anillin RNAi cells was 0.65 ± 0.31 and 0.66 ± 0.34 μm/sec, respectively, indicating there were no changes in microtubules growth. Since the decrease in microtubules after anillin-depletion was most obvious in the central region of the cell near the equatorial cortex (Figure 9; Frenette et al. 2012), EB1 tracks were measured in this region (Figure 10). Interestingly, in anillin RNAi cells (n = 14), there was a significant decrease in the number of long microtubules (> 6 μm) near the equatorial cortex compared to control cells (n= 10; Figure 10). Microtubules longer than 11 μm were never observed in anillin-depleted

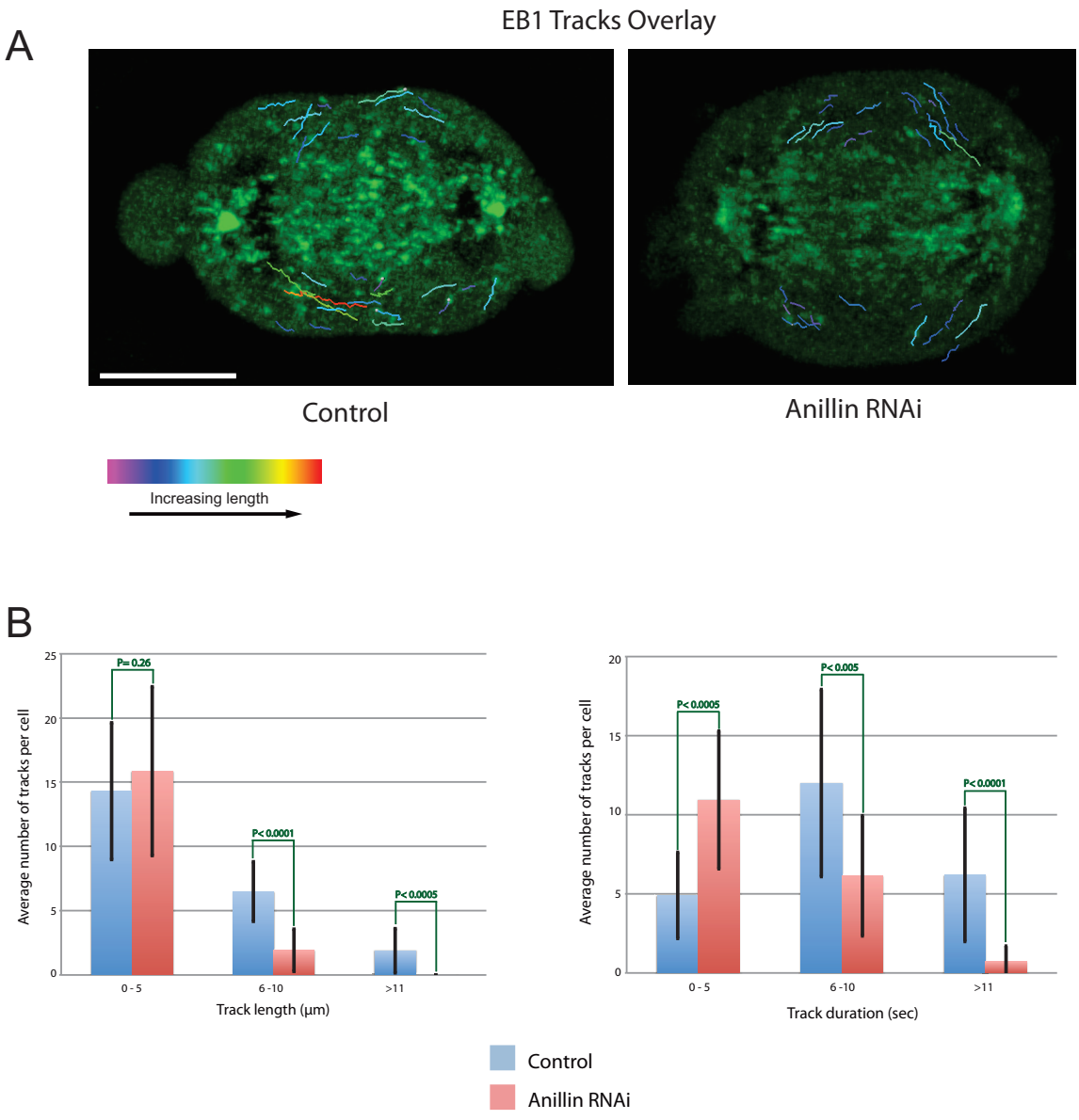

Figure 10. Anillin stabilizes microtubules near the cortex during anaphase.

A) HeLa cells stably expressing EB1:2EGFP were imaged live during mitosis. Z-stack projections of a control and an anillin RNAi cell are shown for a single time point during late anaphase. EB1 comet tracks for the region of interest are color-coded by length and are overlayed on the images. The spectrum scale is indicated (e.g. purple and dark blue are short comets, while yellow and red are long comets). The scale bar is 10 µm. B) Bar graphs show the average number of tracks of different lengths or duration per cell (n=10-14 cells). The black lines show standard deviation. Shown in green are *p* values obtained using the student's t-test. There are a lower number of long tracks near the cortex in anillin-depleted cells compared to control cells.

cells, while they were present in the control cells (Figure 10B). These long microtubules typically emanated from the asters and followed along the cortex to the furrow. In addition, consistent with our measurements showing similar EB1 speeds between the anillin RNAi and control cells, the EB1 comets had shorter duration times after anillin depletion (Figure 10B). These results suggest that anillin is required for the stability of microtubules near the equatorial cortex.

3.2.3 Anillin is required for spindle formation in monopolar HeLa cells

Our data supports a role for anillin in stabilizing microtubules, particularly in the central and equatorial regions of mitotic cells. We also determined if anillin is required for stabilizing microtubules in monopolar cells. Monopolar cells do not have true central spindles, as there are no overlapping, antiparallel microtubules. However, after mitotic exit, the accumulation of central spindle proteins at one end of the polarized microtubules, suggests that these parallel microtubules become bundled and stimulate the accumulation of contractile proteins in the overlying cortex (Hu et al. 2008). To generate monopolar cells, they are first treated with S-trityl-L-cysteine, a drug that inhibits centrosomal separation and causes them to arrest in prometaphase. Then, they are treated with a Cdk1 inhibitor, such as Purvalanol A (Hu et al. 2008), which causes them to exit mitosis. Microtubules polarize towards one side of the cell, where central spindle complexes accumulate at their plus ends and activate RhoA in the overlying cortex. To characterize changes in monopolar spindle microtubules after anillin depletion, we fixed HeLa monopolar cells, co-stained them for anillin (red) and Plk1 (green), and counted the number of

Plk1 cortical foci (to reflect the amount of polarized microtubules; Figure 11). Monopolar cells depleted of anillin had a reduced number of Plk1 foci compared to control cells (Figure 11). Similar to our previous assay measuring changes in tubulin fluorescence, anillin RNAi phenocopied MKLP1 RNAi, which also blocked the accumulation of Plk1 (Figure 11). Interestingly, anillin's microtubule-related function is RhoA-independent, since Ect2-depleted cells showed a higher number of Plk1 foci in comparison to control cells, possibly indicating an increase in microtubule bundling (Figure 11B). To determine if anillin mediates this increased microtubule bundling in Ect2 RNAi cells, monopolar cells were co-depleted of anillin and Ect2. In the absence of anillin, very few Plk1 foci were visible, which phenocopied cells co-depleted of MKLP1 and Ect2 (Figure 11). These results strongly support a role for anillin in stabilizing and/or bundling microtubules in monopolar cells. In particular, anillin may influence parallel microtubules that are bundled near the cortex.

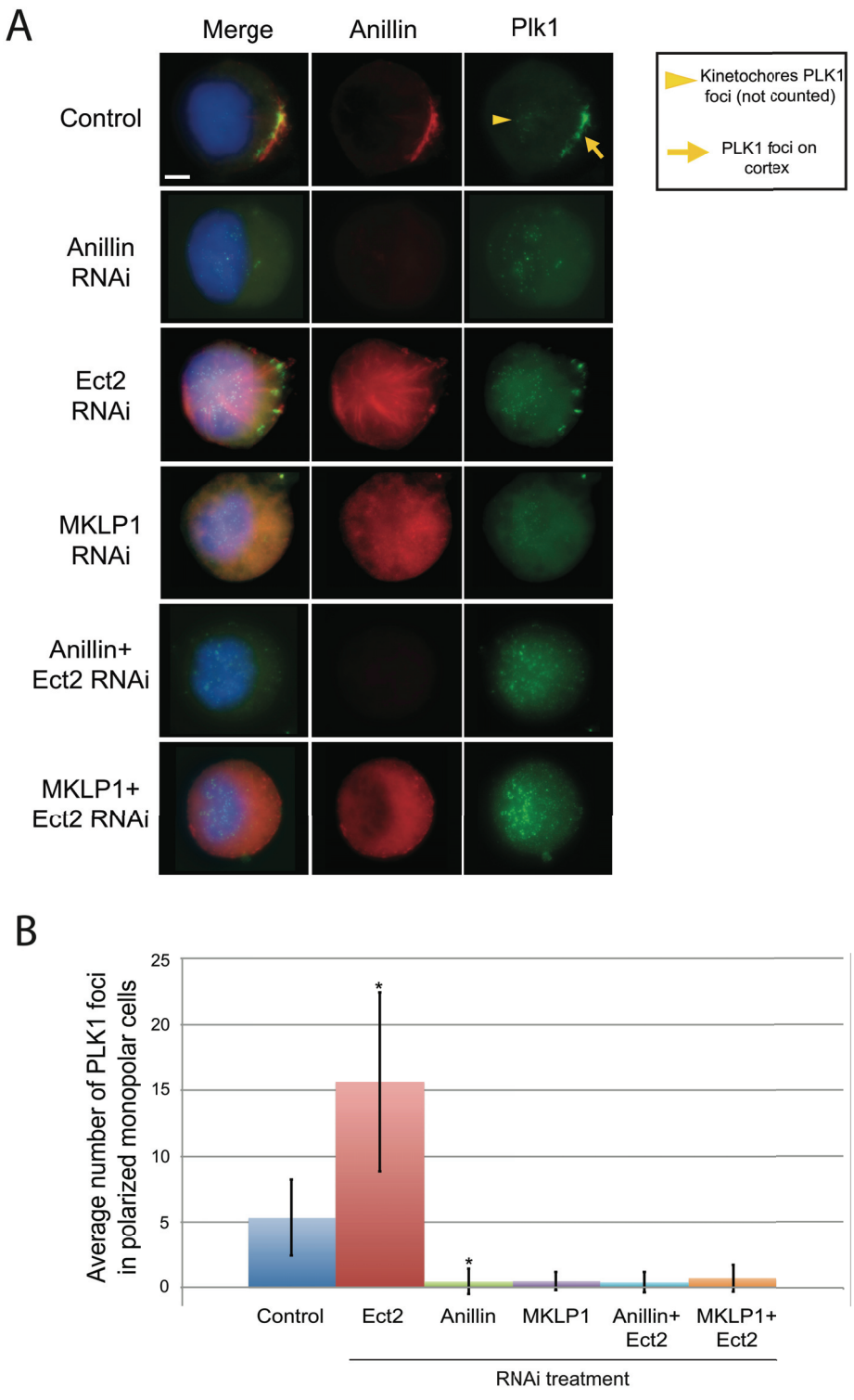

Figure 11. Anillin is required for the accumulation of central spindle proteins in monopolar cells.

A) Z-stack projections of monopolar HeLa cells treated with Ect2, anillin, MKLP1, anillin + Ect2, or MKLP1 + Ect2 RNAi were fixed and co-stained for anillin (red), Plk1 (green) and DNA (DAPI; blue). HeLa cells were arrested in

metaphase with STC (2 mM), then forced to exit mitosis by treatment with Purvalanol A (22.5 μM) and fixed after 20-25 minutes. The yellow arrowhead points to Plk1 foci at kinetochores, and the yellow arrow points to Plk1 foci at the cortex (microtubule-associated and larger in appearance). Anillin and Plk1 channels are shown separately for all cells. Plk1 cortical foci are visible in control and Ect2-depleted cells, but not in any of the other RNAi conditions. The scale bar is 10 μm. (B) A bar graph shows the average number of Plk1 cortical foci for control and RNAi-treated cells from A (n = 24-41 cells per condition). The black bars show standard deviation. *Statistically significant as per the student t-test (p<0.01). Anillin RNAi phenocopies the loss of a central spindle protein (MKLP1), suggesting that it is required for central spindle stability and/or bundling.

Chapter 4. Discussion

We describe an interaction between anillin and microtubules during mitosis. Our data suggests that one of the functions of this interaction may be to maintain the stability of microtubules near the cleavage furrow. Anillin directly binds to microtubules *in vitro* and weakly localizes to microtubules in mitotic HeLa cells (Figures 3 and 8). This localization is much stronger when the levels of active RhoA are reduced or when the stability of microtubules is increased. Furthermore, the interaction between anillin and microtubules may be phosphoregulated by Aurora B kinase. Since equatorially positioned microtubules signal to activate RhoA in the overlying cortex, we propose that anillin's ability to stabilize these cortical microtubules provides feedback between the cortex and the mitotic spindle (Figure 12). This communication between the contractile ring back to the mitotic spindle allows them to coordinately change their position in response to cues and minor perturbations, to ensure that the division plane is maintained between the segregating chromosomes.

4.1 Anillin localizes to microtubules in HeLa cells

During mitosis, anillin localizes more strongly to microtubules before high levels of active RhoA are generated in the cell (e.g. during metaphase and early anaphase), and again after levels of active RhoA drop during late telophase. Prior to RhoA activation, anillin's localization to astral microtubules could be part of

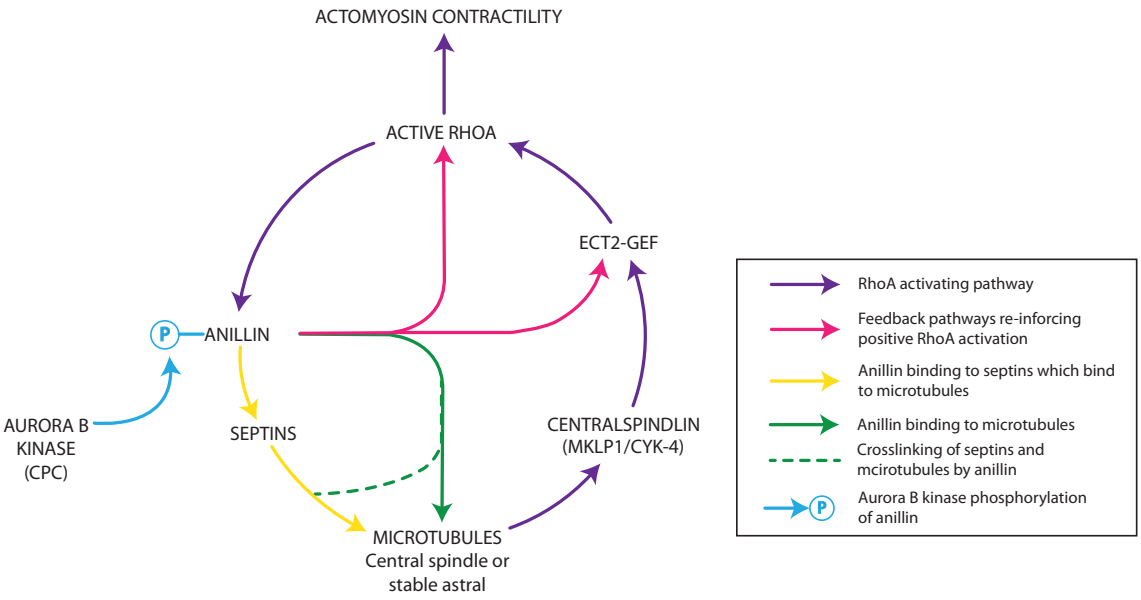

Figure 12. Anillin-microtubule interactions provide feedback from the cortex to the central spindle

A schematic shows the pathway that regulates contractile ring formation. Although anillin is 'downstream' of active RhoA (shown by purple arrows) it may positively feedback to further enhance the RhoA pathway for contractile ring formation by stabilizing RhoA localization at the equatorial cortex, or via regulating Ect2, the GEF that activates RhoA (shown by pink arrows; Frenette et al., 2012). Our data shows that anillin may stabilize equatorially-positioned microtubules, which could contribute to RhoA activation (shown by green arrow). The interaction between anillin and microtubules could be regulated by Aurora B (blue arrow) kinase and could involve crosslinking of septins to microtubules (dashed green line).

sequestration mechanism to prevent the cortical accumulation of contractile proteins before the segregation of sister chromatids. This could be particularly important to ensure that the timing of contractile ring formation and ingression is tied to DNA segregation. After the levels of active RhoA drop in late telophase, anillin is observed on central spindle microtubules as they transition into the midbody. Previous studies showed that in addition to stabilizing the contractile ring, anillin also may be required for midbody formation during cytokinesis (Kechad et al. 2012). During the transition of the central spindle into the midbody, anillin could mediate a 'handoff' of the cytokinetic ring from the plasma membrane to the midbody microtubules (Kechad et al. 2012). This model could be modified to indicate that the interaction between anillin and microtubules could increase the efficiency of this transition.

We found that high levels of active RhoA compete with microtubules for anillin localization. Anillin may form different complexes with its many binding partners (e.g. anillin-septins-RhoA vs. anillin-myosin-actin; Piekny & Maddox 2010). The binding site for microtubules likely lies in the C-terminus of anillin, since this region sufficiently binds to microtubules *in vitro* (Figure 8). This region also contains the binding sites for RhoA, Ect2 and septins. The absence of active RhoA could free microtubule-binding domains normally masked by anillin-RhoA interactions. Anillin's affinity for RhoA likely is higher vs. microtubules, which would permit anillin to respond quickly to changes in the levels of active RhoA. As a key regulator of contractile ring formation, it is important that anillin closely follows the localization of active RhoA.

Anillin may have a higher affinity for stable microtubules. Anillin localizes strongly to taxol-stabilized microtubules, as well as to central spindle microtubules in the absence of active RhoA. We do not think that taxol itself is inducing anillin precipitation, because our *in vitro* co-sedimentation assay shows little anillin pelleting with taxol-supplemented buffer in the absence of microtubules (Figure 8; see section 3.1.6). Furthermore, of the proteins we tested, the only other protein that shows a similar localization pattern in taxol-treated cells is septin 2 (Haji Bik and Piekny, unpublished observations). Septins can also interact with microtubules and may regulate their growth and stability (Surka et al. 2002; Bowen et al. 2011; Sellin et al. 2011). This could point toward a unique function for the anillin-septin complex, which is described later.

4.2 Anillin interacts directly with microtubules

Human anillin directly interacts with microtubules, similar to the *C. elegans* homologue ANI-1 (Tse et al. 2011). We found that although the N-terminus of anillin weakly co-sedimented with microtubules, the C-terminus of anillin bound to microtubules more strongly. This data suggests that the main microtubule-interacting region of anillin is in the C-terminus, although it does not rule out the possibility of a weak site in the N-terminus. There are no consensus sequences for microtubule binding domains *per se,* but they may preferentially interact with stretches of polybasic residues with a high pI (Cravchik et al. 1994). There are several polybasic stretches in anillin, and one stretch in the C-terminus also contains a consensus site for Aurora B (Figure 7B; see section 3.1.5). To further narrow down

the microtubule-binding site, additional co-sedimentation assays could be performed using smaller C-terminal anillin fragments.

Although anillin is able to bind directly to microtubules *in vitro*, it may require additional proteins to localize to microtubules *in vivo*. There are many MAPs that could bridge anillin's interaction to astral microtubules during metaphase and early anaphase. However, during telophase, anillin's localization to centrally located microtubules may be dependent on the centralspindlin complex or the CPC. *Drosophila* anillin binds to RacGAP50C (the homologue of the centralspindlin complex component Cyk4; D'Avino et al. 2008; Gregory et al. 2008). However, human anillin may not bind to Cyk4 (Frenette et al. 2012). Furthermore, human anillin's localization to central spindle microtubules is enriched in the absence of Ect2, suggesting that its microtubule localization is Ect2-independent. Indeed, our data suggests that the CPC could be required for anillin's microtubule interaction *in vivo* (see section 3.1.4 and 3.1.5).

4.3 Anillin associates with microtubules in an Aurora B-dependent manner.

As described earlier, within 20 minutes, anillin's localization strongly shifts from the cortex to taxol-stabilized microtubules. Aurora B kinase and other components of the CPC remain associated with the ends of taxol-stabilized microtubules and Aurora B is required for anillin's localization to these microtubules. Upon Aurora B kinase inhibition using hesperadin, anillin dissociated from taxol-stabilized microtubules and returned to the equatorial cortex (Figure 7A). Aurora B kinase consensus phosphorylation sites usually contain the core

sequence R/K X S/T, and are typically surrounded by basic residues. Aurora B substrates often have multiple sites that can be phosphorylated simultaneously (Andrews et al. 2004; Guse et al. 2005). A scan of anillin's amino acid sequence suggests that there could be multiple Aurora B sites in anillin (Figure 7B). Of particular interest is a site contained in a highly basic region of anillin from 891-907 (Figure 7B). A comparison of lysates collected from cells treated with hesperadin vs. control cells could help determine if anillin is phosphorylated by Aurora B kinase. Cells could also be synchronized for mitosis to enrich the proportion of anillin that is phosphorylated. Furthermore, cells could be transfected with C-terminal constructs containing potential sites, and the sites could be mutated to determine changes in their response to hesperadin.

The CPC could regulate anillin's microtubule localization in a manner other than via Aurora B phosphorylation. The CPC has a dynamic localization pattern during mitosis: it localizes to the centromeres from prophase to metaphase, then localizes to the central spindle and equatorial cortex during anaphase and telophase, and finally localizes to the midbody during abscission (Ruchaud et al. 2007; Carmena et al. 2009). Since the CPC localizes to microtubules and to the cortex during anaphase, one of the CPC components could directly bind to anillin and promote anillin's association with microtubules near the cortex. During later stages of mitosis, as the CPC moves to the midbody, it could help anillin's role in midbody formation by directly interacting with anillin and promoting its localization to microtubules.

4.4 Anillin stabilizes a sub-set of microtubules during cytokinesis

Previous studies showed that anillin is required to stabilize microtubules near the equatorial cortex (Frenette et al. 2012). We also found that the entire central pool of microtubules is lower in anillin-depleted cells in comparison to control cells or Ect2-depleted cells (Figure 9). Interestingly, this phenotype was similar to that observed after the depletion of MKLP1, a component of the centralspindlin complex that is required for central spindle formation (Mishima et al. 2002; Mishima et al. 2004). We further demonstrated a role for anillin in regulating microtubule stability using live cells stably expressing EB1:2EGFP, a plus tip marker for polymerizing microtubules. In comparison to control cells, anillin-depleted cells had fewer long EB1 tracks and an increase in short EB1 tracks (Figures 10A and 10B). The pool of microtubules that seemed to be affected the most were the long microtubules that emanate from the asters and follow along the cortex to the equatorial region. One hypothesis is that some of these microtubules become stable equatorial astral microtubules that are bundled by centralspindlin and recruit Ect2 to activate RhoA (Foe & von Dassow 2008). Anillin could crosslink these microtubules to the cortex and help promote their association with Ect2-centralspindlin complexes.

We observed two distinct phenotypes in anillin-depleted cells (A. Piekny, unpublished observations). The 'oscillating' phenotype likely is caused by the lateral destabilization of the contractile ring, where contractile proteins initially accumulate in the equatorial plane, but then uncouple from RhoA and move around the cortex (Piekny & Glotzer 2008). The second phenotype is a strong cytokinetic

failure, where contractile proteins weakly accumulate in the equatorial plane, but likely do not reach sufficient levels to initiate ingression. These two phenotypes likely reflect different threshold requirements for anillin, and stronger anillin depletion may block the feedback required for stabilizing RhoA activation. In support of this, EB1:2EGFP-expressing cells displaying the oscillation phenotype had a higher number of long-lasting comets (>11 sec) then the non-oscillating cells ($p<0.01$; results not shown). (There may be changes in length between the two phenotypes as well, but it was not statistically significant and a higher n for each phenotype is likely needed.) Therefore, having even a few longer microtubules in the equatorial plane may be sufficient to stabilize RhoA.

Some of the long EB1 tracks that were missing in anillin-depleted cells typically ran close to the plasma membrane and follow along the membrane to the equatorial region. As described earlier, anillin also binds to membrane-associated septins, and both localize to microtubules after enhancing their stability using taxol-treatment (Figure 5; Kinoshita et al. 2002). Recently, septin filaments were shown to act as spatial guides for polymerizing microtubules in polarizing epithelial cells (Bowen et al. 2011). An attractive model is that anillin-septin filaments have a similar role during cytokinesis, and guide long astral microtubules toward the equatorial cortex where they are stabilized and bound by centralspindlin complexes. The same study by Bowen et al. (2011) also showed a dramatic decrease in bundled microtubules in septin-depleted cells. Interestingly, we similarly observed a loss of bundled microtubules in anillin-depleted monopolar cells (Figure 11). We also saw what appeared to be an increase in bundled microtubules when

anillin localized to central spindle microtubules in Ect2-depleted monopolar or bipolar cells (Figure 11). This would be consistent with a model in which anillin and septins work together to promote microtubule stability or bundling (Figure 12). Since septin filaments show high redundancy from one heterocomplex to another, it is difficult to assess direct requirements for septins in regulating microtubules (Mostowy & Cossart 2012). To further understand how septins and anillin regulate microtubules, we could perform live imaging of EB1:2EGFP in combination with mCherry-labelled septin 2 or septin 7 in control vs. anillin-depleted cells. Furthermore, *in vitro* microtubule bundling assays could be performed with a purified septin complex (e.g. 2, 6 and 7) and anillin, separately or in combination.

Lastly, previous studies using the same EB1:2EGFP construct report speeds of 0.32 ± 0.12μm/sec in interphase HeLa cells (Matov et al. 2010), which is lower than our results (see section 3.2.2). Faster EB1 speeds are expected in mitotic cells, since microtubule dynamics are enhanced to permit both the formation and modeling of the mitotic spindle to capture and segregate sister chromatids (Li et al. 2011). However, the differences between our speeds and those previously reported could be due to differences in manual tracking vs. automated tracking using specialized software such as plus-Tip Tracker (Matov et al. 2010).

To summarize, anillin can directly interact with microtubules and localizes to microtubules during mitosis. Anillin may preferentially localize to stable microtubules, which may be regulated by Aurora B kinase. Furthermore, anillin's localization to microtubules is typically competed by active RhoA. Anillin's interaction with microtubules may be required to stabilize a specific population of

cortical microtubules during anaphase and removing anillin causes the loss of these microtubules that contribute to RhoA activation and cytokinetic failure.

References

Adams, R., Maiato, H., Earnshaw, W.C., & Carmena, M., 2001. **Essential roles of Drosophila inner Centromere protein (INCENP) and Aurora B in histone H3 phosphorylation, metaphase chromosome alignment, kinetochore disjunction, and chromosome segregation.** *The Journal of cell biology*, 153: 865–879.

Andrews, P.D., Ovechkina, Y., Morrice, N., Wagenbach, M., Duncan, K., Wordeman, L. & Swedlow, J.R., 2004. **Aurora B regulates MCAK at the mitotic centromere.** *Developmental cell*, 6: 253–68.

Bement, W.M., Benink, H. & von Dassow, G., 2005. **A microtubule-dependent zone of active RhoA during cleavage plane specification.** *The Journal of cell biology*, 170: 91–101.

Bement, W.M., Miller, A.L. & von Dassow, G., 2006. **Rho GTPase activity zones and transient contractile arrays.** *BioEssays : news and reviews in molecular, cellular and developmental biology*, 28: 983–93.

Bertin, A., McMurray, M., Thai, L., Garcia, G., Votin, V., Grob, P., Allyn, T., Thorner, J. & Nogales, E., 2010. **Phosphatidylinositol-4,5-bisphosphate promotes budding yeast septin filament assembly and organization.** *Journal of molecular biology*, 404: 711–31.

Bieling, P., Telley, I. & Surrey, T., 2010. **A minimal midzone protein module controls formation and length of antiparallel microtubule overlaps.** *Cell*, 142: 420–32.

Biron, D., Alvarez-Lacalle, E., Tlusty, T. & Moses, E., 2005. **Molecular Model of the Contractile Ring.** *Physical Review Letters*, 95: 098102_1-4

Bowen, J.R., Hwang, D., Bai, X., Roy, D. & Spiliotis, E.T., 2011. **Septin GTPases spatially guide microtubule organization and plus end dynamics in polarizing epithelia.** *The Journal of cell biology*, 194: 187–97.

Brennan, I.M. Peters, U., Kapoor, T.M. & Straight, A.F., 2007. **Polo-like kinase controls vertebrate spindle elongation and cytokinesis.** *PloS one*, 2: e409.

Bringmann, H. & Hyman, A., 2005. **A cytokinesis furrow is positioned by two consecutive signals.** *Nature*, 436: 731–4.

Burkard, M.E. Randall, C.L., Larochelle, S., Zhang, C., Shokat, K.M., Fisher, R.P. & Jallepalli, P.V., 2007. **Chemical genetics reveals the requirement for Polo-like kinase 1 activity in positioning RhoA and triggering cytokinesis in human cells.** *Proceedings of the National Academy of Sciences of the United States of America*, 104: 4383–8.

Canman, J., Cameron, L., Maddox, P., Straight, A., Tirnauer, J.S., Mitchison, T.J., Fang, G., Kapoor, T.M., & Salmon, E.D., 2003. **Determining the position of the cell division plane.** *Nature*, 424: 1074–1078.

Carmena, M., Ruchaud, S. & Earnshaw, W.C., 2009. **Making the Auroras glow: regulation of Aurora A and B kinase function by interacting proteins.** *Current opinion in cell biology*, 21: 796–805.

Cheeseman, I.M., Anderson, S., Jwa, M., Green, E.M., Kang, J.S., Yates, J.R., Chan, C.S.M., Drubin, D.G. & Barnes, G., 2002. **Phospho-regulation of kinetochore-microtubule attachments by the Aurora kinase Ipl1p.** *Cell*, 111: 163–72.

Cravchik, A., Reddy, D. & Matus, A., 1994. **Identification of a novel microtubule-binding domain in microtubule-associated protein 1A (MAP1A).** *Journal of cell science*, 107: 661–72.

D'Avino, P.P., Takeda, T., Capalbo, L., Zhang, W., Lilley, K.S., Laue, E.D. & Glover, D.M., 2008. **Interaction between Anillin and RacGAP50C connects the actomyosin contractile ring with spindle microtubules at the cell division site.** *Journal of cell science*, 121: 1151–8.

Dechant, R. & Glotzer, M., 2003. **Centrosome separation and central spindle assembly act in redundant pathways that regulate microtubule density and trigger cleavage furrow formation.** *Developmental cell*, 4: 333–44.

Derry, W.B., Wilson, L. & Jordan, M., 1995. **Substoichiometric binding of taxol suppresses microtubule dynamics.** *Biochemistry*, 34: 2203–11.

Douglas, M.E., Davies, T., Joseph, N. & Mishima, M., 2010. **Aurora B and 14-3-3 Coordinately Regulate Clustering of Centralspindlin during Cytokinesis.** *Current biology* 20: 927–933.

Eggert, U.S., Mitchison, T.J. & Field, C.M., 2006. **Animal cytokinesis: from parts list to mechanisms.** *Annual review of biochemistry*, 75: 543–66.

Estey, M.P., Di Ciano-Oliveira, C., Froese, C.D., Bejide, M.T. & Trimble, W.S., 2010. **Distinct roles of septins in cytokinesis: SEPT9 mediates midbody abscission.** *The Journal of cell biology*, 191: 741–9.

Euteneuer, U. & Mcintosh, J.R., 1980. **Polarity of Midbody and Phragmoplast.** *The Journal of cell biology*, 87: 509–515.

Field, C.M., Coughlin, M., Doberstein, S., Marty, T. & Sullivan, W., 2005. **Characterization of anillin mutants reveals essential roles in septin localization and plasma membrane integrity.** *Development* 132: 2849–60.

Field, C.M. & Alberts, B.M., 1995. **Anillin, a contractile ring protein that cycles from the nucleus to the cell cortex.** *The Journal of cell biology*, 131: 165–78.

Foe, V.E. & von Dassow, G., 2008. **Stable and dynamic microtubules coordinately shape the myosin activation zone during cytokinetic furrow formation.** *The Journal of cell biology*, 183: 457–70.

Frenette, P., Haines, E., Loloyan, M., Kinal, M., Pakarian, P. & Piekny, A., 2012. **An anillin-Ect2 complex stabilizes central spindle microtubules at the cortex during cytokinesis.** *PloS one*, 7: e34888.

Gaillard, J., Neumann, E., Van Damme, D., Stoppin-Mellet, V., Ebel, C., Barbier, E., Geelen, D. & Vantard, M., 2008. **Two Microtubule-associated Proteins of Arabidopsis MAP65s Promote Antiparallel Microtubule Bundling**. *Molecular biology of the cell*, 19: 4534–4544.

Glotzer, M., 2009. **The 3Ms of central spindle assembly: microtubules, motors and MAPs.** *Nature reviews: Molecular cell biology*, 10: 9–20.

Glotzer, M., 2005. **The molecular requirements for cytokinesis.** *Science ,* 307: 1735–9.

Green, R., Paluch, E. & Oegema, K., 2012. **Cytokinesis in animal cells.** *Annual review of cell and developmental biology*, 28: 29–58.

Gregory, S.L., Ebrahimi, S., Milverton, J., Jones, W.M., Bejsovec, A. & Saint, R., 2008. **Cell division requires a direct link between microtubule-bound RacGAP and Anillin in the contractile ring.** *Current biology,* 18: 25–9.

Guse, A., Mishima, M. & Glotzer, M., 2005. **Phosphorylation of ZEN-4/MKLP1 by aurora B regulates completion of cytokinesis.** *Current biology* 15: 778–86.

Hickson, G.R.X. & O'Farrell, P.H., 2008. **Anillin: a pivotal organizer of the cytokinetic machinery.** *Biochemical Society transactions*, 36: 439–41.

Hu, C.-K., Coughlin, M., Field, C.M. & Mitchison, T.J., 2008. **Cell polarization during monopolar cytokinesis.** *The Journal of cell biology*, 181: 195–202.

Hu, C.-K., Coughlin, M., Field, C.M. & Mitchison, T.J, 2011. **KIF4 regulates midzone length during cytokinesis.** *Current biology*, 21: 815–24.

Inoue, Y.H., Savoian, M.S., Suzuki, T., Máthé, E., Yamamoto, M.-T. & Glover, D.M., 2004. **Mutations in orbit/mast reveal that the central spindle is comprised of two microtubule populations, those that initiate cleavage and those that propagate furrow ingression.** *The Journal of cell biology*, 166: 49–60.

Jordan, M. & Wilson, L., 2004. **Microtubules as a target of anticancer drugs.** *Nature Reviews Cancer*, 4: 253–265.

Kechad, A., Jananji, S., Ruella, Y. & Hickson, G.R.X., 2012. **Anillin acts as a bifunctional linker coordinating midbody ring biogenesis during cytokinesis.** *Current biology,* 22: 197–203.

Kimura, K., Tsuji, T., Takada, Y., Miki, T. & Narumiya, S., 2000. **Accumulation of GTP-bound RhoA during cytokinesis and a critical role of ECT2 in this accumulation.** *The Journal of biological chemistry*, 275: 17233–6.

Kinoshita, M., Kumar, S Mizoguchi, A., Ide, C., Kinoshita, A., Haraguchi, T., Hiraoka, Y. & Noda, M., 1997. **Nedd5, a mammalian septin, is a novel cytoskeletal component interacting with actin-based structures.** *Genes & Development*, 11: 1535–1547.

Kinoshita, M. Field, C.M., Coughlin, M., Straight, A. & Mitchison, T.J., 2002. **Self- and actin-templated assembly of Mammalian septins.** *Developmental cell*, 3: 791–802.

Kovar, D.R., 2006. **Molecular details of formin-mediated actin assembly.** *Current opinion in cell biology*, 18: 11–7.

Lewellyn, L., Dumont, J., Desai, A. & Oegema, K., 2010. **Analyzing the effects of delaying aster separation on furrow formation during cytokinesis in the Caenorhabditis elegans embryo.** *Molecular biology of the cell,* 21: 50–62.

Lewellyn, L., Carvalho, A., Desai, A., Maddox, A.S. & Oegema, K., 2011. **The chromosomal passenger complex and centralspindlin independently contribute to contractile ring assembly.** *The Journal of cell biology*, 193: 155–69.

Li, W., Miki, T., Watanabe, T., Kakeno, M., Sugiyama, I., Kaibuchi, K. & Goshima, G., 2011. **EB1 promotes microtubule dynamics by recruiting Sentin in Drosophila cells.** *The Journal of cell biology*, 193: 973–83.

Liu, J., Fairn, G.D., Ceccarelli, D.F., Sicheri, F. & Wilde, A., 2012. **Cleavage furrow organization requires PIP(2)-mediated recruitment of anillin.** *Current biology,* 22: 64–9.

Ma, X., Kovács, M., Conti , M.-A., Wang A., Zhang, Y., Sellers, J.R. & Adelsteina, R.S., 2012. **Nonmuscle myosin II exerts tension but does not translocate actin in**

vertebrate cytokinesis. *Proceedings of the National Academy of Sciences of the United States of America*, 109: 4509–14.

Maddox, A.S., Habermann, B., Desai, A. & Oegema, K., 2005. **Distinct roles for two C. elegans anillins in the gonad and early embryo.** *Development,* 132: 2837–48.

Maddox, A.S., Lewellyn, L., Desai, A. & Oegema, K.,2007. **Anillin and the septins promote asymmetric ingression of the cytokinetic furrow.** *Developmental cell*, 12: 827–35.

Matov, A., Applegate, K., Kumar, P., Thoma, C., Krek, W., Danuser, G. & Wittmann, T., 2010. **Analysis of microtubule dynamic instability using a plus-end growth marker.** *Nature methods*, 7: 761–8.

Matsumura, F., 2005. **Regulation of myosin II during cytokinesis in higher eukaryotes.** *Trends in cell biology*, 15: 371–7.

Mimori-Kiyosue, Y., Shiina, N. & Tsukita, S., 2000. **The dynamic behavior of the APC-binding protein EB1 on the distal ends of microtubules.** *Current biology,* 10: 865–8.

Mishima, M., Kaitna, S. & Glotzer, M., 2002. **Central spindle assembly and cytokinesis require a kinesin-like protein/RhoGAP complex with microtubule bundling activity.** *Developmental cell*, 2: 41–54.

Mishima, M., Pavicic, V., Grüneberg, U., Nigg, E. & Glotzer, M., 2004. **Cell cycle regulation of central spindle assembly**. *Nature*, 430: 0–5.

Morrison, E.E., Wardleworth, B.N., Askham, J.M., Markham, F. & Meredith, D.M., 1998. **EB1, a protein which interacts with the APC tumour suppressor, is associated with the microtubule cytoskeleton throughout the cell cycle.** *Oncogene*, 17: 3471–7.

Mostowy, S. & Cossart, P., 2012. **Septins: the fourth component of the cytoskeleton.** *Nature reviews: Molecular cell biology*, 13: 183–94.

Murthy, K. & Wadsworth, P., 2008. **Dual role for microtubules in regulating cortical contractility during cytokinesis.** *Journal of cell science*, 121: 2350–9.

Nishimura, Y. & Yonemura, S., 2006. **Centralspindlin regulates ECT2 and RhoA accumulation at the equatorial cortex during cytokinesis.** *Journal of cell science*, 119: 104–14.

Oegema, K. & Mitchison, T.J., 1997. **Rappaport rules: Cleavage furrow induction in animal cells.** *Proceedings of the National Academy of Sciences of the United States of America*,94: 4817-20.

Oegema, K., Savoian, M.S., Mitchison, T.J. & Field, C.M., 2000. **Functional analysis of a human homologue of the Drosophila actin binding protein anillin suggests a role in cytokinesis.** *The Journal of cell biology*, 150: 539–52.

Ozlü, N., Monigatti, F., Renard, B.Y., Field, C.M., Steen, H., Mitchison, T.J. & Steen, J.J., 2010. **Binding partner switching on microtubules and aurora-B in the mitosis to cytokinesis transition.** *Molecular & cellular proteomics*, 9: 336–50.

Pavicic-Kaltenbrunner, V., Mishima, M., & Glotzer, M., 2007. **Cooperative assembly of CYK-4/MgcRacGAP and ZEN-4/MKLP1 to form the centralspindlin complex.** *Molecular biology of the cell*, 18: 4992–5003.

Petronczki, M. Glotzer, M., Kraut, N. & Peters, J.-M., 2007. **Polo-like kinase 1 triggers the initiation of cytokinesis in human cells by promoting recruitment of the RhoGEF Ect2 to the central spindle.** *Developmental cell*, 12: 713–25.

Pfau, S.J. & Amon, A., 2012. **Chromosomal instability and aneuploidy in cancer: from yeast to man.** *EMBO reports*, 13: 515–27.

Piekny, A., Werner, M. & Glotzer, M., 2005. **Cytokinesis: welcome to the Rho zone.** *Trends in cell biology*, 15: 651–8.

Piekny, A.J. & Glotzer, M., 2008. **Anillin is a scaffold protein that links RhoA, actin, and myosin during cytokinesis.** *Current biology,* 18: 30–6.

Piekny, A.J. & Maddox, A.S., 2010. **The myriad roles of Anillin during cytokinesis.** *Seminars in cell & developmental biology*, 21: 881–91.

Pollard, T.D., 2004. **Ray Rappaport Chronology: Twenty-Five Years of Seminal Papers on Cytokinesis in the Journal of Experimental Zoology.** *Journal of experimental zoology,* 301A: 9-14

Ruchaud, S., Carmena, M. & Earnshaw, W.C., 2007. **Chromosomal passengers: conducting cell division.** *Nature reviews: Molecular cell biology*, 8: 798–812.

Saito, S., Tatsumoto, T., Lorenzi, M.V., Chedid, M., Kapoor, V., Sakata, H., Rubin, J. & Miki, T.,2003. **Rho exchange factor ECT2 is induced by growth factors and regulates cytokinesis through the N-terminal cell cycle regulator-related domains.** *Journal of cellular biochemistry*, 90: 819–36.

Salmon, E.D., Leslie, R.J., Saxton, W.M., Karow, M.L. & McIntosh, J.R., 1984. **Spindle microtubule dynamics in sea urchin embryos: analysis using a fluorescein-labeled tubulin and measurements of fluorescence redistribution after laser photobleaching.** *The Journal of cell biology*, 99: 2165–74.

Saxton, W.M., Stemple, D.L., Leslie, R..J, Salmon, E.D., Zavortink, M. & McIntosh, J.R., 1984. **Tubulin dynamics in cultured mammalian cells.** *The Journal of cell biology*, 99: 2175–86.

Sellin, M.E., Holmfeldt, P., Stenmark, S. & Gullberg, M., 2011. **Microtubules support a disk-like septin arrangement at the plasma membrane of mammalian cells.** *Molecular biology of the cell*, 22: 4588–601.

Sessa, F., Mapelli, M., Ciferri, C., Tarricone, C., Areces, L.B., Schneider, T.R., Stukenberg, P.T. & Musacchio, A., 2005. **Mechanism of Aurora B activation by INCENP and inhibition by hesperadin.** *Molecular cell*, 18: 379–91.

Sisson, J.C., Field, C.M., Ventura, R., Royou, A. & Sullivan, W., 2000. **Lava lamp, a novel peripheral golgi protein, is required for Drosophila melanogaster cellularization.** *The Journal of cell biology*, 151: 905–18.

Somers, W.G. & Saint, R., 2003. **A RhoGEF and Rho family GTPase-activating protein complex links the contractile ring to cortical microtubules at the onset of cytokinesis.** *Developmental cell*, 4:29–39.

Straight, A., Field, C.M. & Mitchison, T.J., 2005. **Anillin binds nonmuscle myosin II and regulates the contractile ring.** *Molecular biology of the cell*, 16: 193–201.

Surka, M.C., Tsang, C.W. & Trimble, W.S., 2002. **The Mammalian Septin MSF Localizes with Microtubules and Is Required for Completion of Cytokinesis.** *Molecular biology of the cell,* 13: 3532–3545.

Suzuki, C,. Daigo, Y., Ishikawa, N., Kato, T., Hayama, S., Ito, T., Tsuchiya, E. & Nakamura, Y., 2005. **ANLN plays a critical role in human lung carcinogenesis through the activation of RHOA and by involvement in the phosphoinositide 3-kinase/AKT pathway.** *Cancer research*, 65: 11314–25.

Tanaka-Takiguchi, Y., Kinoshita, M. & Takiguchi, K., 2009. **Septin-mediated uniform bracing of phospholipid membranes.** *Current biology,* 19: 140–5.

Tse, Y.C., Piekny, A. & Glotzer, M., 2011. **Anillin promotes astral microtubule-directed cortical myosin polarization.** *Molecular biology of the cell*, 22: 3165–75.

Verbrugghe, K.J.C. & White, J.G., 2007. **Cortical centralspindlin and G alpha have parallel roles in furrow initiation in early C. elegans embryos.** *Journal of cell science*, 120: 1772–8.

Werner, M., Munro, E. & Glotzer, M., 2007. **Astral signals spatially bias cortical myosin recruitment to break symmetry and promote cytokinesis.** *Current biology*, 17: 1286–97.

Wolfe, B., Takaki, T., Petronczki, M. & Glotzer, M., 2009. **Polo-like kinase 1 directs assembly of the HsCyk-4 RhoGAP/Ect2 RhoGEF complex to initiate cleavage furrow formation.** *PLoS biology*, 7: e1000110.

Yüce, O., Piekny, A. & Glotzer, M., 2005. **An ECT2-centralspindlin complex regulates the localization and function of RhoA.** *The Journal of cell biology*, 170: 571–82.

Zhao, W. & Fang, G., 2005. **MgcRacGAP controls the assembly of the contractile ring and the initiation of cytokinesis.** *Proceedings of the National Academy of Sciences of the United States of America*, 102: 13158–63.